STRUCTURAL CONNECTIVITY OF AN INTEROCEPTION NETWORK IN SCHIZOPHRENIA

By

Beier Yao

A DISSERTATION

Submitted to
Michigan State University
in partial fulfillment of the requirements
for the degree of

Psychology–Doctor of Philosophy

2022

ABSTRACT

STRUCTURAL CONNECTIVITY OF AN INTEROCEPTION NETWORK IN SCHIZOPHRENIA

By

Beier Yao

Interoception refers to the processing, integration, and interpretation of bodily signals by the brain. Interoception is key to not only basic survival, but also many cognitive processes, especially motivational and affective functioning. There is emerging evidence suggesting altered interoception in schizophrenia, but its neural underpinning has not been examined. The current study aims to investigate the structural connectivity of a putative interoception network in schizophrenia, and its relationship with affective functioning and clinical symptoms. Thirty-five participants with schizophrenia (SZ) and 36 healthy control participants (HC) underwent diffusion tensor imaging (DTI) and performed tasks measuring emotional functioning. Probabilistic tractography was used to identify white matter tracts connecting the key hubs forming the interoception network (i.e., rostral and caudal anterior cingulate cortex, ventral anterior insula, dorsal mid and posterior insula, and amygdala). Microstructural integrity of these tracts was compared across groups and correlated with measures of emotional functioning and symptom severity. I found that SZ exhibited altered structural connectivity in the putative interoception network, compared to HC. The structural connectivity of the network was correlated with emotion recognition in HC, supporting a link between the interoception network and emotional functioning. However, this correlation was much weaker in SZ, suggesting less reliance on this network. I did not find a correlation between the structural connectivity and clinical symptoms in SZ. These findings suggest that altered interoception may play a role in illness mechanisms of schizophrenia, especially in relation to emotional deficits.

ACKNOWLEDGEMENTS

I would like to thank Dr. Katy Thakkar for her guidance and support, Dr. Jason Moser, Dr. Mark Becker, and Dr. Alexander Johnson for their helpful feedback, Dr. Ivy Tso for generously sharing her data with me, my parents and friends for always believing in me, Yemo Duan for making sure I am fed and get enough sleep, my cats for providing constructive distractions and meaningful companionship, and all the participants for their participation.

TABLE OF CONTENTS

LIST OF TABLES

LIST OF FIGURES

INTRODUCTION

Schizophrenia is a severe mental illness that affects 1 in every 100 individuals in the world. It is ranked the 15th leading cause of disability worldwide (Vos et al., 2017). Persons with schizophrenia struggle daily with a disconcerting disconnect between the actual world and their perceived world in the forms of vivid and frightening hallucinations (false perceptions without external stimuli) and bizarre delusions (irrational beliefs that persist despite conflicting evidence). Moreover, they suffer from chronically low motivation, anxiety, decreased ability to concentrate, and physical illnesses due to medication side effects. The average life expectancy of individuals with schizophrenia falls 20 years below that of the general population (Laursen, Nordentoft, & Mortensen, 2014), and 1 in every 10 dies by suicide (Sher & Kahn, 2019). The illness leaves most unemployed, and many homeless, in prisons, and without social support. The human and economic costs of schizophrenia are staggering. Even with pharmacological and psychosocial treatments, the recovery rate remains regrettably low: only 1 in every 7 individuals with schizophrenia can lead an independent life with minimal residual symptoms (Jaaskelainen et al., 2013), with even fewer reaching their full potential. Current treatments for schizophrenia fall short because illness mechanisms are largely unknown: we don't know exactly what it is that we are treating.

Research into the physiological mechanisms of schizophrenia has traditionally focused almost exclusively on how the brain processes and interprets information from the *outside* world. For example, it has long been established that perceptual disturbances (from subtle distortions to outright hallucinations) are prevalent in persons with schizophrenia, and have been theorized to have downstream consequences that potentially lead to altered thought processes and clinical symptoms (Maher, 2005; Silverstein, 2016). However, there is growing evidence that *internal*

signals from the body can influence a wide range of brain functions, including basic perception, processing speed, reasoning, emotion, motivation, and our sense of self (Makowski, Sperduti, Blondé, Nicolas, & Piolino, 2020; Pramme, Larra, Schächinger, & Frings, 2014, 2016; Tsakiris & De Preester, 2019). The processing of such bodily signals by the central nervous system is called interoception. Disrupted interoception may underlie a wide range of symptoms of schizophrenia. For example, one may develop the delusional sense of something ominous impending when there is no clear explanation to intense bodily sensations. On the other hand, losing touch with one's bodily sensations may lead to the delusion that one is not in control of their own body. Over time, the constant sense of uncertainty around the cause of bodily sensations may lead to a generalized sense of low self-efficacy (Stephan et al., 2016). This may further develop into negative symptoms such as reduced level of activity and social isolation, as an attempt to minimize changes in bodily sensations and consequently low self-efficacy. Therefore, the proposed study aims to understand the brain network for interoception in schizophrenia as a potential illness mechanism.

Allostasis, interoception, and emotion

The most important function of the brain is, arguably, to keep the animal alive (Schulkin & Sterling, 2019; Sterling, 2012). To do that efficiently, the brain engages in a predictive regulation process – allostasis. This idea stands in contrast with the conventional view of "homeostasis", which posits that the brain tries to keep all internal systems within certain "set points" (e.g., a narrow range of normal body temperature) for healthy functioning, and only initiates regulatory actions when a system deviates from its set point. However, the allostasis model posits that this kind of regulation is inefficient and can hardly meet an animal's changing energy needs in a natural environment. Rather, the more energy-efficient mechanism is to

constantly predict the metabolic needs that may arise in the next moment and adjust and prepare the body accordingly (e.g., drink before we feel thirsty, put on gloves before we get frostbite).

A formal computational account of the allostatic process in the brain has been developed based on the predictive coding framework - the interoceptive inference theory (Barrett & Simmons, 2015; Seth & Friston, 2016; Seth, Suzuki, & Critchley, 2012). The theory posits that the brain maintains an internal model of the body and is constantly trying to minimize any discrepancies between the model and actual signals from the internal milieu. Specifically, the brain generates top-down predictions of the state of the body based on past experience and the external environment, while the body generates bottom-up signals detailing the actual state of the body at the moment. A mismatch between the two will form a prediction error signal that the brain will then try to minimize. To minimize prediction error signals, the brain will either shift the prediction to match the incoming sensory data (i.e., update the model of the body), or shift the sensory data towards the prediction (i.e., change the sensory input through hormonal, visceral, immunological, and autonomic mechanisms or behavior; Seth, 2015). This latter way of reconciling prediction errors is referred to as active inference.

The interoceptive inference theory has important implications for one's affective experience (Barrett, 2017; Seth, 2013). Within this framework, emotion has been proposed to be the conscious product of resolving interoceptive prediction errors through active inference (i.e., shifting sensory data towards the prediction; Barrett, 2017). For example, when you are preparing to give a public presentation, your brain predicts that your body will need more energy and sends out such autonomic commands to different bodily systems. At the same time, your brain also sends out interoceptive predictions of potential sensory input: you may feel your heart beating faster, your face getting warmer, your hands shaking, your throat feeling dry, etc. At the

conscious level, the combined pattern of these interoceptive sensory signals may bear the name of "excited," "anxious," "embarrassed," or "nervous" in different situations. The ultimate interpretation of this pattern in this particular instance depends on your prediction, which is heavily informed by previous situations where you have experienced similar emotions. As you continue to give the presentation, your body may experience changes that may be consistent or inconsistent with your predicted pattern of interoceptive signals. What you "feel" emotionally may change accordingly as well, as you incorporate new prediction errors, regulate your body differently, or shift your attention elsewhere. As your emotional state changes, you may also decide to adopt different behavioral strategies to better accommodate your allostatic needs (e.g., if you are feeling too anxious, you may decide to take a pause and drink some water to calm yourself down). In other words, emotion is a "constructed concept" for conscious description of the consequences of active interoceptive inference (Barrett, 2017). It is not the same as interoceptive predictions (as many of them are unconscious and too localized and specific to single organs and receptors), but a more abstract conscious "label" that enables us to prepare for bodily sensations and decide on adaptive actions when in need. This also explains why we may have slightly different patterns of bodily sensations for the same emotion, as well as the same pattern of bodily signals for different emotions, because emotion emerges through a dynamic process that incorporates information over multiple sources (i.e., interoception, context, past experience, attentional focus) and is therefore vague and flexible by nature.

So far, there is limited data on the biological basis of the interoceptive inference process, but multiple theories have been proposed detailing potential pathways involved (Barrett & Simmons, 2015; Smith, Thayer, Khalsa, & Lane, 2017). The Embodied Predictive Interoceptive Coding (EPIC) model proposed a detailed account of how interoceptive predictions and

prediction errors may transmit within the central nervous system (Barrett & Simmons, 2015). Specifically, the model proposed that the agranular visceromotor cortices (including cingulate, posterior ventral medial prefrontal cortex, posterior orbitofrontal cortex, and ventral anterior insula) are the key brain structures for estimating the allostatic needs of the body, based on current resources and past experience. Specifically, they generate autonomic, hormonal, and immunological commands to adjust how corresponding systems function in accordance with the body's needs. At the same time, these regions are argued to send out interoceptive predictions of the expected sensations resulting from such allostatic changes over the body to the primary interoceptive sensory cortex – the mid-to-posterior insular cortex. Then the actual interoceptive afferent signals travel up to be compared with the predicted signals to compute the prediction error. These prediction errors are then propagated back to the visceromotor regions where the predictions originated. Notably, tract-tracing studies in monkeys and recent neuroimaging studies in humans confirmed the existence of an intrinsic allostatic-interoceptive system in the brain (Kleckner et al., 2017). Moreover, individuals with stronger functional connectivity within this network also exhibited higher accuracy perceiving their own bodily states, further supporting the EPIC model.

Altered interoception in schizophrenia

A large body of physiological evidence *suggests* altered interoception (and allostasis) in schizophrenia, such as reduced pain sensitivity (see Stubbs et al., 2015 for a meta-analysis), altered regulation of body temperature (see Chong & Castle, 2004 for review), and reduced baseline heart rate variability (natural beat-to-beat fluctuations in heart rate; see Clamor, Lincoln, Thayer, & Koenig, 2016 for a meta-analysis). Surprisingly, only four studies have *directly* examined interoception in schizophrenia based on psychophysiological task performance. All

four studies found that individuals with schizophrenia were less able to detect their own heartbeats (Ardizzi et al., 2016; Critchley et al., 2019; Koreki, Funayama, Terasawa, Onaya, & Mimura, 2020; Torregrossa, Amedy, Roig, Prada, & Park, 2022). However, the validity of this heartbeat detection task to measure interoception was recently called into question as accumulating evidence suggests that participants can base their estimation of number of heartbeats within a time interval on prior knowledge and beliefs about heart rate rather than actual heartbeat sensations (Brener & Ring, 2016; Ring & Brener, 2018). Therefore, poor heartbeat detection in schizophrenia patients as measured using this task may not necessarily reflect altered interoceptive accuracy.

Altered interoception could be caused by alterations in both peripheral and central nervous systems. Unlike the relatively understudied peripheral nervous system, there is a robust evidence base for abnormalities in key regions within the central interoception network, especially the insula cortex: persons with schizophrenia have decreased gray-matter volume, reduced cortical thickness, abnormal cellular structure, and altered expression of certain proteins related to neuronal plasticity in the insula (see Wylie & Tregellas, 2010 for review). Rapid atrophy of the right insula during the first episode has been found to correlate with less improvement in positive symptoms later on, while subtle atrophy of the left insular in chronic patients were correlated with more severe negative symptoms (Takahashi et al., 2020). Though insula functioning during interoception hasn't been directly examined in persons with schizophrenia, abnormal response in insula has been observed in other tasks that are potentially related to interoception, such as the processing of emotional facial expressions (see Wylie & Tregellas, 2010 for review).

Likewise, structural and functional abnormalities have been identified in other brain

regions theorized to be key components of the interoception network (Barrett & Simmons, 2015). There is an established link between reduced gray matter volume in anterior cingulate cortex and the onset of schizophrenia (see Bersani et al., 2014 for review) and poorer functional outcome (see Wojtalik, Smith, Keshavan, & Eack, 2017 for review). There is also some evidence suggesting that cingulate hypoactivity is related to negative symptoms (see Bersani et al., 2014 for review). Persons with schizophrenia also exhibit deficits in subregions of ventromedial prefrontal cortex dedicated to value-based decision making and social cognition (Hiser & Koenigs, 2018), and interoception has been theorized as playing an important role in both processes (Gu & FitzGerald, 2014; Ondobaka, Kilner, & Friston, 2017).

As a first step towards understanding the potential involvement of the interoception network in the development of schizophrenia, the current study investigated the structural connectivity of a putative interoception network and its relationship with affective functioning and clinical symptoms in schizophrenia. I predicted that relative to healthy controls, participants with schizophrenia would have reduced structural connectivity and reduced white matter microstructural integrity within the interoception network. I also predicted that structural connectivity within this network would be correlated with emotional functioning across participants and with clinical symptom severity in schizophrenia. Findings from this study will add to our knowledge of interoception in schizophrenia and may have implications for novel illness mechanisms and treatment targets.

METHODS

Overview

In the current study, I 1) compared structural connectivity of the interoception network in participants with schizophrenia (SZ) and healthy controls (HC) using diffusion tensor imaging (DTI) and probabilistic tractography; 2) assessed relationships between interoception network connectivity and emotional functioning in all participants; 3) assessed relationships between interoception network connectivity and positive and negative symptoms in SZ.

Participants

I recruited 37 individuals with a diagnosis of either schizophrenia or schizoaffective disorder (SZ) from an outpatient psychiatric facility and through community and internet advertisements. Thirty-six HC without a personal history of past or current mental illness and without first-degree relatives with a history of psychotic disorders were recruited through community and internet advertisements and existing subject pools. Diagnoses were determined using the Structured Clinical Interview for DSM-IV. Chlorpromazine (CPZ) equivalent antipsychotic dosages were calculated in SZ (Andreasen, Pressler, Nopoulos, Miller, & Ho, 2010).

Exclusion criteria included a history of closed head injury, significant medical or neurological illness, substance abuse within the one month prior to study, substance dependence within the six months prior to study, and vision that was not normal or corrected-to-normal. All participants gave written informed consent and were reimbursed for participation. The study was approved by the University of Michigan Medical School Institutional Review Board, and determined as not involving “human subjects” by the Human Research Protection Program of the Michigan State University (STUDY00003128).

Assessments

Positive and negative symptoms were assessed using the Scale for the Assessment of Positive Symptoms (SAPS; Andreasen, 1984b) and Scale for the Assessment of Negative Symptoms (SANS; Andreasen, 1984a), respectively. Overall psychiatric symptom severity was measured by Brief Psychiatric Rating Scale (BPRS; Overall & Gorham, 1962). All participants completed the Penn Emotion Recognition - 40 Task (ER40; Gur et al., 2002) and Mayer-Salovey-Caruso Emotional Intelligence Test (MSCEIT; Mayer, Salovey, & Caruso, 1999) to assess their emotional functioning. The ER40 measures facial emotion recognition. In this task, participants were asked to judge the emotion of 40 photographs of faces, choosing among five response options: anger, sadness, fear, joy, and no emotion. The total accuracy score was used in all statistical analyses. The MSCEIT is a performance-based battery that measures participants' emotional intelligence through 141 multiple-choice questions. Here, participants are asked to solve emotional problems based on typical everyday scenarios and stimuli, rather than providing subjective evaluations of their own emotional skills. The battery consists of four subscales: perceiving emotions (e.g., judging the emotion of photographs of faces), using emotions to facilitate cognitive processes (e.g., judging how helpful certain emotions may be in specific scenarios), understanding emotions (e.g., judging how emotions may change and progress in interpersonal interactions), and managing emotions (e.g., judging how helpful certain actions may be in regulating one's emotion). Participants' accuracy scores were then compared to the normative data to generate standardized scores. The total standardized score was used in all statistical analyses to reduce the number of statistical tests since I do not have specific hypotheses regarding specific subscales.

Image acquisition

All DTI data were acquired at the University of Michigan on a 3.0 T GE Discovery MR750 scanner (LX [8.3] release, General Electric Healthcare, Buckinghamshire, United Kingdom) with a 32-channel receiver array head coil and a multi-band slice accelerated echo-planar imaging (EPI) sequence. Diffusion-weighted scans were acquired twice along opposite phase-encoding directions (primary direction: anterior-posterior; reversed direction: posterior-anterior) with 96 noncollinear gradient directions distributed over 4 different b-values (b = 500, 1,000, 2,000, and 3,000 s/mm^2), covering the entire brain (Repetition Time (TR) = 4,100 ms; Echo Time (TE) = minimum; field of view = 24 cm; slice thickness = 1.7 mm; no slice gap; axial slices; matrix size 140 × 140). A total of at least 6 images without diffusion weighting (b = 0 s/mm^2) were collected for all participants, interleaved within the entire scanning sequence, while for approximately half of the participants, 6 additional b = 0 images were collected at the beginning of the sequence. For registration purposes, a whole-brain three-dimensional T1-weighted scan (SPGR, TR = 2850 ms; TI = 1060 ms; TE = 2.3 ms; flip angle = 8°; field of view, 25.6 cm; voxel size: 0.8 mm × 0.8mm × 0.8 mm; parallel acceleration factor = 2) was acquired.

Preprocessing

The neuroimaging data was organized in the BIDS format (Gorgolewski et al., 2016). The preprocessing (i.e., denoising, eddy current-induced distortion and head motion correction) and quality control of the diffusion-weighted scans was performed using MRtrix3 (Tournier et al., 2019). Two diffusion-weighted scans were acquired along reversed phase-encoding directions to improve spatial distortion correction. A brain mask was also created from bias corrected diffusion-weighted images. For quality assurance, a percent of outlier slices (due to head motion, eddy current distortion, etc.) was calculated for each participant. Head movements

were quantified using mean head translation and rotation in the x, y, and z directions and absolute and relative total displacement (except for translation in the phase-encoding direction). Group differences in percent of outlier slices and head movement parameters were examined using independent T-tests.

Regions of interest

Based on the EPIC model (Barrett & Simmons, 2015) and the recent study that identified the functional allostatic-interoceptive network (Kleckner et al., 2017), the current study included the following six regions of interest (ROIs) in each hemisphere: rostral anterior cingulate cortex (rACC), caudal anterior cingulate cortex (cACC), amygdala, ventral anterior insula (vaIns), dorsal mid insula (dmIns), and dorsal posterior insula (dpIns). According to the EPIC model, interoceptive prediction signals travel from rACC, cACC, amygdala, and vaIns to dmIns and dpIns, while interoceptive prediction error signals travel the opposite direction (**Figure 1**). Therefore, the white matter pathways connecting these ROIs are the key structures supporting the dynamic process of interoceptive inference.

Each participant's structural T1-weighted image was automatically segmented and parcellated into known cortical and subcortical structures using Freesurfer 6.0 (http://surfer.nmr.mgh.harvard.edu). Corresponding segmentations formed the rACC, cACC, and amygdala ROIs in each hemisphere. Because Freesurfer parcellations do not contain subdivisions within the insular cortex, the Brainnetome probabilistic atlas was used to generate the vaIns, dmIns, and dpIns ROIs in the standard (Montreal neuroimaging; MNI) space (Fan et al., 2016). The subdivisions were generated based on structural connectivity patterns, and the insular subdivisions correspond well to the underlying cytoarchitectonic structure.

To transform all ROIs into the native space for diffusion analysis, each participant's T1-

weighted image was first coregistered with their mean *b*0 image using SPM 12 (http://www.fil.ion.ucl.ac.uk/spm/software/spm12). Next, transformation matrices were derived for each participant by registering their T1-weighted images to the Freesurfer conformed space using *bbregister* (Greve & Fischl, 2009). The inverse of these registration matrices was then applied to transform the Freesurfer ROIs (i.e., rACC, cACC, and amygdala) to diffusion space. Lastly, normalization coefficient maps were generated for each participant by normalizing their T1-weighted images to the MNI space using the FSL 6.0.3 (FMRIB Software Library; www.fmrib.ox.ac.uk/fsl). The inverse warping parameters from this step were then used to transform the MNI ROIs (i.e., vaIns, dmIns, and dpIns) to the native space. All transformed ROIs were visually examined in the native space for quality assurance (**Figure 2**, Top panel).

Probabilistic tractography

Probabilistic tractography was performed using FSL 6.0.3 (FMRIB's Software Library, www.fmrib.ox.ac.uk/fsl). Probabilistic tractography is an analysis technique that reconstructs anatomical pathways, presumably white matter tracts, between any given brain regions based on a distribution profile of probable fiber orientations in each voxel (Behrens, Berg, Jbabdi, Rushworth, & Woolrich, 2007; Behrens et al., 2003). Within each hemisphere, probabilistic tractography was conducted using the *probtrackx2* command between the visceromotor control regions (rACC, cACC, amygdala, and vaIns) and the interoceptive sensory regions (dmIns and dpIns), so that one ROI served as a seed (start point) while the other ROI served as a target (end point). In other words, I did not run probabilistic tractography between any two visceromotor control regions (e.g., rACC to amygdala), or between dmIns and dpIns. The distribution profile of probabilistic connectivity is computed by iteratively sending out a huge number of streamlines from the seed area, going in a direction drawn from a probabilistic distribution of the principal

diffusion direction in each voxel, until it is determined structurally impossible for a white matter tract to continue. Only streamlines that reached the target were included in the analysis, and streamlines were not allowed to continue after reaching the target. In addition, the mid-sagittal plane was used as an exclusion mask to avoid streamlines travelling into the other hemisphere (Landman et al., 2012; Mori & van Zijl, 2002; Mori & Zhang, 2006). The other ROIs not serving as the seed or target were also included in the exclusion mask to avoid streamlines wandering through multiple ROIs before reaching the target. I modeled two crossing fibers per voxel. All resulting tracts were visually examined for quality assurance.

For each participant, two outcome measures were generated at the end of the tractography process for each ROI pair within each hemisphere: (1) total streamlines and (2) constructed tracts with a connectivity value within each voxel of the tract. I describe how each measure is derived and what they reflect below.

The measure of total streamlines refers to the sum of all streamlines sent from a seed that eventually reaches the target. Therefore, a higher value indicates stronger structural connectivity between an ROI pair. Because DTI cannot distinguish the direction of axonal fibers, measures generated from both directions (e.g., rACC to dmIns and dmIns to rACC) were considered equally accurate and combined to achieve a single measure of total streamlines for each ROI pair. This resulted in 8 measures in total (i.e., vaIns – dmIns, vaIns – dpIns, amygdala – dmIns, amygdala – dpIns, rACC – dmIns, rACC – dpIns, cACC – dmIns, cACC – dpIns) for each hemisphere. Tracts were constructed for each seed-target pair based on the connectivity value at each voxel of the brain. Voxels with higher numbers indicate a higher probability that this voxel is part of the tract between the seed and target regions. Tracts starting from both directions were

considered equally accurate and combined to achieve a single tract for each ROI pair. This resulted in 8 tracts in total per hemisphere.

In order to perform group analyses, these measures were further corrected and standardized. Numbers of streamlines are not only determined by actual structural connectivity, but also influenced by other factors like size of the seed ROI (i.e., bigger seeds send out more streamlines). Thus, higher connectivity values in a given tract do not necessarily indicate a larger probability of an actual structural connection there. That is, the number of streamlines passing through a given voxel cannot be compared across seed/target combinations or individuals. To control for differences in connectivity value due to individual differences in brain size, the measures of total streamlines were corrected by the ROI sizes (i.e., divided by the sum of the number of voxels within each pair of ROIs).

To make sure only white matter structures were included in tract-based analysis, I used each individual's whole-brain white matter map as a mask to preserve only connectivity values within these voxels. Tissue segmentation was performed on T1-weighted images by using MRtrix3 (Tournier et al., 2019). The white matter map was then generated by including only voxels where the probability of the tissue being white matter was higher than the probability of the tissue being grey matter or CSF. After applying the white matter masks, I then corrected the connectivity values within each voxel of the tract by dividing the value by the sum of total streamlines between the corresponding pair of ROIs. These tracts were then transformed to MNI space and averaged within each group. Tracts were thresholded using the 99^{th} percentile of all voxels within the tract. These thresholded connectivity maps for each ROI pair were then binarized into masks within each group for later analysis and extraction of diffusivity measures.

Diffusivity measures of microstructural integrity

Each participant's diffusion-weighted images were fit to a tensor model using FSL 6.0.3 (FMRIB's Software Library, www.fmrib.ox.ac.uk/fsl) to generate four diffusivity maps, each with one of the following diffusivity measures at each voxel: fractional anisotropy (FA), mean diffusivity (MD), axial diffusivity (AD), and radial diffusivity (RD). FA quantifies the overall anisotropy within a voxel (i.e., how prominent the principal diffusion direction is). MD quantifies the average diffusivity along all directions within a voxel. AD characterizes diffusion along the principal axis, while RD characterizes average diffusion along the directions perpendicular to the principal (axial) direction. FA is currently the most widely used measure of anisotropy, highly sensitive to microstructural integrity of white matter tracts. Higher FA value means higher anisotropy and lower diffusivity. However, FA value contains no information on the orientation of anisotropy and thus can be difficult to interpret in isolation. A decrease in FA could be caused by multiple factors: white matter neuropathology, fiber crossing, and normal aging (Alexander, Lee, Lazar, & Field, 2007). Therefore, it is recommended to use multiple diffusivity measures for better understanding of the microstructure of white matter. Specifically, RD appears to be a more sensitive indicator of myelination, while AD seems to indicate axonal degeneration (Song et al., 2002). Higher values on these diffusivity measures mean higher diffusivity along those directions. MD seems to be best at assessing white matter maturation and aging (Abe et al., 2002; Snook, Plewes, & Beaulieu, 2007). Higher MD value means higher diffusivity overall.

For each participant, diffusivity maps were normalized to MNI space so that diffusivity measures could be extracted from each of the binarized group tracts to be averaged and used in

later analysis. Whole-brain white matter integrity was quantified by averaging diffusivity measures within each participant's whole-brain white matter map.

Statistical analyses

Statistical analyses were performed using IBM SPSS Statistics 25.0 (IBM, Armonk, NY) and R (R Core Team, Vienna, Austria). Age was included as a covariate in all group comparisons as white matter integrity decreases with age.

First, to make sure that the group tracts occupy similar locations in the brain between HC and SZ, I computed η^2 for all pairs (HC and SZ) of binarized group tract masks, as well as for the network mask that combines all tract masks in one image (Cohen et al., 2008). η^2 measures the similarity between two images on a voxel-by-voxel basis. The value ranges from 0 (no similarity) to 1 (identical). I hypothesized that some tracts may have a lower η^2, but across all tracts, η^2 would be moderately high. Consequently, η^2 for the network mask may fall in the moderate range.

Next, to examine group differences in structural connectivity of the interoception network, I compared both connectivity strength and microstructural integrity. To compare connectivity strength, I conducted a MANCOVA on the 16 corrected total streamline values to protect against inflated Type I error rate due to multiple comparisons (Tabachnick & Fidell, 2013). Because many of the corrected total streamline measures were not normally distributed, a log transformation was performed to achieve normal distribution. Group was included as a between-subjects variable, hemisphere was included as a within-subjects variable, and age was included as a covariate. Significant main effects were followed up by univariate tests. Individual group comparisons of total streamlines between each ROI pair were evaluated with a repeated-measures ANCOVA, including diagnostic group as a between-subjects variable, hemisphere as a

within-subjects variable, and age as a covariate. Significant effects of group were followed up with independent T-tests, and significant effects of hemisphere were followed up with paired T-tests. I hypothesized that SZ would have lower connectivity strength than HC within the putative interoception network.

To compare microstructural integrity of the white matter tracts, I conducted MANCOVAs on FA and MD, including group as a between-subjects variable, hemisphere as a within-subjects variable, and age as a covariate. Similarly, significant main effects were followed up by univariate tests and T-tests. I hypothesized that SZ would have lower FA and higher MD than HC, reflecting compromised white matter microstructure. To explore the nature of putative group differences, for those tracts in which significant group differences in FA or MD were observed, I conducted follow-up analyses on RD and AD. Because I do not have specific hypotheses regarding the exact nature of the white matter abnormality in SZ, the analyses on RD and AD were exploratory. To make sure that any putative group differences in these diffusivity measures were specific to the interoception network, I also conducted independent T-tests on FA, MD, RD, and AD averaged across individual participant's whole-brain and per hemisphere white matter maps. There were no group differences in any of the measures (p ranged from .33 - .98). I also conducted repeated-measures ANOVAs to identify potential group by hemisphere interaction effects in whole-brain white matter diffusivity. I found no such interactions in any of the measures (p ranged from .16 to .75, partial η^2 ranged from 0.001 to 0.03). Therefore, whole-brain diffusivity measures were not controlled for in these analyses.

Finally, to assess whether structural connectivity of the interoception network is associated with emotional functioning, I investigated the relationship between FA and performance on ER40 and MSCEIT in all participants. To reduce the number of statistical tests, I

did not include the other diffusivity measures or the streamline measure in this analysis. Since I am interested in the specific influence of structural connectivity within the interoception network, mean FA over the whole brain was regressed out of the tract FA measurements. These standardized residuals were used in the remaining analyses. These "standardized FA values" are 0 when equal to the whole brain FA average, higher for more anisotropic tracts and lower for more isotropic tracts. When no hemisphere effect was found in group comparisons, standardized FA values were computed by regressing whole-brain FA out of the tract FA averaged across both hemispheres. When lateralized effects were observed, mean FA within each hemisphere was regressed out of the corresponding tract FA. For standardized FA from each tract, I ran linear regression models that can be expressed in the following regression equation, where *i* stands for the tract, and *j* stands for the emotional functioning task (ER40 accuracy score or MSCEIT total score):

$$Standardized\ FA_i = \beta_0 + \beta_1(Diagnostic\ Group) + \beta_2\left(Emotion\ Task_j\right) + \beta_3\left(Diagnostic\ Group \times Emotion\ Task_j\right)$$

Group was dummy coded as 0 = HC and 1 = SZ. In other words, HC served as the implicit reference group in the model. ER40 accuracy score and MSCEIT total score were grand mean centered. I hypothesized that lower FA within a putative interoception network would be related to worse emotional functioning.

Using SZ data only, I examined the relationship between clinical symptom severity and structural connectivity of the interoception network. For this analysis, only tracts with significant group differences were included. I calculated Spearman's rank correlation coefficients (r_s) between SAPS and SANS total scores (sum of individual symptom ratings) and global summary

scores (sum of global item ratings) and standardized FA from tracts that differed in connectivity between the two groups. I hypothesized that lower FA would be related to more severe symptoms.

Because most participants with schizophrenia recruited for the study were taking antipsychotics, I also examined potential confounding effects of antipsychotic use by correlating the normalized (chlorpromazine equivalent) dose (Andreasen et al., 2010; Danivas & Venkatasubramanian, 2013; Rothe, Heres, & Leucht, 2018) with diffusivity measures of microstructural integrity and emotional functioning measures.

RESULTS

Two participants were excluded due to poor imaging data quality (one due to scanner acquisition error and the other due to excessive Gibbs' ringing artifacts on the T1-weighted image). The remaining participants (35 SZ, 36 HC) did not differ significantly in percent of outlier slices and head movement parameters (**Table S1**). The two groups did not differ significantly on age, sex, race, ethnicity, parental education, and premorbid IQ (**Table 1**).

Group differences in structural connectivity

The thresholded group tracts within the putative interoception network can be seen in **Figure 2**. I computed $\boldsymbol{\eta}^2$ for all pairs of binarized group tracts and the entire network to examine overall similarities between the location of the tracts. Results show that the tracts share very similar locations between the two groups ($\boldsymbol{\eta}^2$ ranged from 0.80 to 0.94 for all tracts; network $\boldsymbol{\eta}^2$ = 0.88), indicating no gross anatomical differences in the location of the putative interoception network between SZ and HC.

Next, to compare connectivity strength, I conducted a MANCOVA on the corrected total streamline measures using group as a between-subjects variable, hemisphere as a within-subjects variable, and age as a covariate (**Figure 3**). The MANCOVA revealed a significant hemisphere effect ($F(8,62) = 27.27$, $p < .001$; Wilk's $\Lambda = 0.22$, partial $\eta^2 = 0.78$) and a significant group × hemisphere interaction effect ($F(8,62) = 2.99$, $p = .007$; Wilk's $\Lambda = 0.72$, partial $\eta^2 = 0.28$). There was no significant group effect ($F(8,61) = 1.15$, $p = .34$; Wilk's $\Lambda = 0.87$, partial $\eta^2 = 0.13$) or age effect ($F(8,61) = 1.62$, $p = .14$; Wilk's $\Lambda = 0.83$, partial $\eta^2 = 0.18$). Follow-up univariate tests revealed that the group × hemisphere interaction effect was significant in the rACC-dmIns tract ($F(1,69) = 11.44$, $p = .001$, partial $\eta^2 = 0.14$), amygdala-dmIns tract ($F(1,69) = 4.29$, $p = .04$, partial $\eta^2 = 0.06$), and vaIns-dpIns tract ($F(1,69) = 6.64$, $p = .01$, partial $\eta^2 = 0.09$).

Post-hoc T-tests revealed that HC had higher connectivity values than SZ in the right rACC-dmIns tract ($t(69) = -3.39$, $p = .001$, Cohen's $d = -0.80$) and the left vaIns-dpIns tract ($t(69) = -2.53$, $p = .01$, Cohen's $d = -0.60$), while SZ had higher connectivity values than HC in the left amygdala-dmIns tract ($t(69) = 2.09$, $p = .04$, Cohen's $d = 0.50$). These results indicate a mixed pattern of group differences in structural connectivity within the putative interoception network that are complicated by hemisphere effects. Because hemisphere effects are not the focus of the current study, follow-up analyses on main effects of hemisphere and interactions driven by hemisphere effects (i.e., when the lateralized effect is significantly different between HC and SZ, but the group difference does not differ between hemispheres) are detailed in the Appendix C. Supplementary results.

Lastly, to compare microstructural integrity of the white matter tracts, I conducted two MANCOVAs on FA and MD extracted from each tract, including group as a between-subjects variable, hemisphere as a within-subjects variable, and age as a covariate (**Figure 4**). The MANCOVA on FA revealed significant effects of group ($F(8,61) = 12.23$, $p < .001$; Wilk's $\Lambda = 0.38$, partial $\eta^2 = 0.62$), hemisphere ($F(8,62) = 103.34$, $p < .001$; Wilk's $\Lambda = 0.07$, partial $\eta^2 = 0.93$), group × hemisphere interaction ($F(8,62) = 45.41$, $p < .001$; Wilk's $\Lambda = 0.15$, partial $\eta^2 = 0.85$), and age ($F(8,61) = 3.26$, $p = .004$; Wilk's $\Lambda = 0.70$, partial $\eta^2 = 0.30$). The MANCOVA on MD also revealed significant effects of group ($F(8,61) = 9.96$, $p < .001$; Wilk's $\Lambda = 0.43$, partial $\eta^2 = 0.57$), hemisphere ($F(8,62) = 108.14$, $p < .001$; Wilk's $\Lambda = 0.07$, partial $\eta^2 = 0.93$), and group × hemisphere interaction ($F(8,62) = 173.70$, $p < .001$; Wilk's $\Lambda = 0.04$, partial $\eta^2 = 0.96$); however, there was no significant age effect on MD ($F(8,61) = 1.56$, $p = .16$; Wilk's $\Lambda = 0.83$, partial $\eta^2 = 0.17$). I now go through the tracts between each pair of ROIs one by one to discuss results from follow-up univariate ANCOVA tests.

For the amygdala-dpIns tract, there was a significant group effect on FA ($F(1,68) = 4.04$, $p = .048$, partial $\eta^2 = 0.06$). Post-hoc T-test revealed that SZ had lower FA than HC ($t(69) = -2.01$, $p = .049$, Cohen's $d = -0.48$). There was also a significant group × hemisphere interaction effect on FA ($F(1,69) = 8.13$, $p = .006$, partial $\eta^2 = 0.11$). Post-hoc T-tests revealed that the group difference in FA was only statistically significant in the left hemisphere ($t(69) = -2.63$, $p = .01$, Cohen's $d = -0.62$). For MD, there was no group effect ($F(1,68) = 0.02$, $p = .88$, partial $\eta^2 = 0$). To explore the nature of the group difference in FA, I conducted follow-up group comparisons on AD and RD. There was a significant group effect on AD ($F(1,68) = 11.26$, $p = .001$, partial $\eta^2 = 0.14$), but not on RD ($F(1,68) = 0.78$, $p = .38$, partial $\eta^2 = 0.01$). Post-hoc T-test revealed that SZ had lower AD than HC ($t(69) = -3.24$, $p = .002$, Cohen's $d = -0.77$). There was also a significant group × hemisphere interaction effect on AD ($F(1,69) = 9.24$, $p = .003$, partial $\eta^2 = 0.12$). While the group difference in AD was significant in both hemispheres, it was much larger in the right hemisphere (left: $t(69) = -2.08$, $p = .04$, Cohen's $d = -0.49$; right: $t(69) = -4.00$, $p < .001$, Cohen's $d = -0.95$). In summary, SZ had reduced white matter microstructural integrity than HC in the amygdala-dpIns tract, seemingly driven by reduced diffusivity along the principal axial direction.

For the amygdala-dmIns tract, there was a significant group × hemisphere interaction effect on FA ($F(1,69) = 185.10$, $p < .001$, partial $\eta^2 = 0.73$). Post-hoc T-tests revealed that HC had higher FA than SZ in the left hemisphere ($t(69) = -4.42$, $p < .001$, Cohen's $d = -1.05$), but lower FA than SZ in the right hemisphere ($t(69) = 2.24$, $p = .03$, Cohen's $d = 0.53$). There was also a significant group × hemisphere interaction effect on MD ($F(1,69) = 694.08$, $p < .001$, partial $\eta^2 = 0.91$). Post-hoc T-tests revealed that HC had lower MD than SZ in the left hemisphere ($t(69) = 3.74$, $p < .001$, Cohen's $d = 0.89$), but higher MD than SZ in the right

hemisphere ($t(69) = -3.93$, $p < .001$, Cohen's $d = -0.93$). To explore the nature of the group × hemisphere interaction effect on FA and MD, I conducted follow-up analyses on AD and RD. There was a significant group × hemisphere interaction effect on AD ($F(1,69) = 47.29$, $p < .001$, partial $\eta^2 = 0.41$) and RD ($F(1,69) = 421.92$, $p < .001$, partial $\eta^2 = 0.86$). Post-hoc T-tests revealed that HC had higher AD than SZ, but in the right hemisphere only ($t(69) = -3.98$, $p < .001$, Cohen's $d = -0.95$). On the other hand, HC had lower RD than SZ in the left hemisphere ($t(69) = 3.86$, $p < .001$, Cohen's $d = 0.92$), but higher RD than SZ in the right hemisphere ($t(69) = -3.15$, $p = .002$, Cohen's $d = -0.75$). In summary, there was a mixed pattern in group differences in the structural connectivity within the amygdala-dmIns tract, complicated by hemisphere effects.

For the cACC-dpIns tract, there was no group × hemisphere interaction effect on FA ($F(1,69) = 0.96$, $p = .33$, partial $\eta^2 = 0.01$). For the cACC-dmIns tract, there was no group × hemisphere interaction effect on MD ($F(1,69) = 2.90$, $p = .09$, partial $\eta^2 = 0.04$). For the rACC-dpIns tract, there was no group × hemisphere interaction effect on FA ($F(1,69) = 0.38$, $p = .54$, partial $\eta^2 = 0.005$). For the vaIns-dmIns tract, there was no group × hemisphere interaction effect on FA ($F(1,69) = 0.12$, $p = .73$, partial $\eta^2 = 0.002$).

Lastly, I examined potential confounding effects of antipsychotic use. I found no correlation between the chlorpromazine equivalent dose and any of the diffusivity measures ($-0.33 <$ all r values < 0.29, $.07 <$ all p values $< .98$).

Relationship between structural connectivity and emotional functioning

HC performed significantly better than SZ on both emotional functioning tasks (ER40: $t(68) = -3.37$, $p = .002$, Cohen's $d = -0.82$; MSCEIT: $t(67) = -4.60$, $p < .001$, Cohen's $d = -1.11$). To assess the associations between the structural connectivity of the interoception network and

emotional functioning, I conducted linear regressions using diagnostic group, emotional functioning measures (ER40 accuracy and MSCEIT total score), and group × emotional functioning interaction to predict standardized FA from each tract. Here I only present significant main and interaction effects involving emotional functioning measures. See **Table S2 & S3** for all model coefficients.

MSCEIT total score was a significant predictor of standardized FA from the right vaIns-dmIns tract in HC (b = -0.02, t(65) = -2.28, p = .03), and this association was not significantly different in SZ (b = 0.02, t(65) = 1.22, p = .23). In other words, higher performance on MSCEIT was related with lower than whole-brain FA values in the right vaIns-dmIns tract in both groups.

ER40 accuracy was a significant predictor of standardized FA from the tracts between left rACC and dpIns (b = -0.13, t(66) = -2.11, p = .04), right rACC and dpIns (b = -0.13, t(66) = -2.10, p = .04), left rACC and dmIns (b = -0.13, t(66) = -2.11, p = .04), right rACC and dmIns (b = -0.14, t(66) = -2.33, p = .02), and right cACC and dmIns (b = -0.14, t(66) = -2.44, p = .02) in HC (**Figure 5**). Moreover, these associations were significantly different in SZ (left rACC-dpIns: b = 0.16, t(66) = 2.27, p = .03; right rACC-dpIns: b = 0.19, t(66) = 2.81, p = .007; left rACC-dmIns: b = 0.17, t(66) = 2.57, p = .01; right rACC-dmIns: b = 0.21, t(66) = 3.22, p = .002; right cACC-dmIns: b = 0.16, t(66) = 2.60, p = .01). In other words, higher performance on ER40 was related with lower than whole-brain FA values in multiple tracts within the putative interoception network in HC, but these associations were significantly weaker in SZ.

Lastly, I found no correlation between the chlorpromazine equivalent dose and MSCEIT total score (r = 0.12, p = .53) and ER40 accuracy (r = 0.25, p = .18).

Relationship between structural connectivity and clinical symptoms

Lastly, I conducted Spearman's rank correlation analyses between SAPS and SANS total and global summary scores and standardized FA from tracts that differed in connectivity between the two groups. No correlations were found between the standardized FA and SAPS and SANS total and global summary scores ($-0.22 <$ all r_s values < 0.13; $.20 <$ all p values $< .96$; see **Table S4** for complete results).

DISCUSSION

In this study, I examined the structural connectivity of a putative interoception network in participants with schizophrenia (SZ) and healthy controls (HC). Given interoception's crucial role in supporting emotional functioning, I also examined the relationship between interoception network connectivity and emotional functioning. I found that the spatial location of the network is highly similar between SZ and HC. However, there was a lateralized pattern of white matter alterations in connections within the network in SZ. Group differences in network connectivity were largely specific to the connections between amygdala and insular cortex (dmIns and dpIns). Moreover, I found a correlation between emotion recognition and the microstructural integrity of white matter specific to the putative interoception network in HC, supporting the theory that the putative interoception network is involved in emotional functioning. However, this relationship was significantly weaker in SZ, potentially suggesting less reliance on this network in emotional functioning.

The current finding of increased right amygdala-dmIns structural connectivity in SZ is consistent with a previous finding of increased functional connectivity between right amygdala and insular cortex in persons with schizophrenia, compared to their unaffected relatives (Goswami et al., 2020). The finding of decreased left amygdala-dmIns connectivity in SZ is consistent with a previous finding of reduced white matter microstructural integrity (indexed by lower FA) in the left amygdala-vaIns connection in persons with schizophrenia (Amodio et al., 2018). As Amodio and colleagues divided the insular cortex into anterior and posterior portions (i.e., with no mid-insula) using a different atlas, it is possible that there are overlaps between their anterior insula and the mid insula in the current study.

The combined pattern of group differences in diffusivity measures provides more insights into the underlying mechanisms of potential white matter abnormalities in persons with schizophrenia (Feldman, Yeatman, Lee, Barde, & Gaman-Bean, 2010). Compared to HC, SZ had reduced FA and increased RD in the left amygdala-dmIns white matter pathway; AD did not differ between groups. Such a profile indicates that compromised microstructural integrity in this tract may be driven by myelin and oligodendroglia dysfunction (Bennett, Madden, Vaidya, Howard, & Howard, 2010; Davis et al., 2003). Curiously, the right amygdala-dmIns white matter pathway exhibited almost the exact opposite pattern of group differences (i.e., increased FA, reduced AD, and reduced RD in SZ), potentially suggesting more tightly packed axons with smaller axonal diameter in SZ (Feldman et al., 2010). On the other hand, the pattern of group differences in the left amygdala-dpIns white matter pathway (i.e., reduced FA and AD and unaffected RD in SZ) may indicate mild or early-stage axonal degeneration without demyelination (Song et al., 2003). Given the same directionality in group differences (i.e., reduced connectivity in SZ) in left amygdala-dmIns and amygdala-dpIns tracts, as well as similar patterns in functional connectivity observed in a previous study (Kleckner et al., 2017), I will not differentiate dmIns and dpIns further in the discussion below for the sake of simplicity.

To understand the implications of altered amygdala-insula connectivity in schizophrenia, I will first revisit the role of this connection within the interoception network. The amygdala has numerous reciprocal connections to cortical and subcortical structures that allow it to immediately translate emotionally important input into autonomic and endocrine physiological responses before processed and integrated information can reach the level of conscious awareness (Šimić et al., 2021). It is associated with biological instincts (e.g., thirst, hunger, libido), motivational states, and the activation of fight-or-flight response. On the other hand,

ACC seems to be involved in higher-level processes like using context and event-specific information to regulate autonomic and emotional states (Seamans & Floresco, 2022). Therefore, the combination of decreased amygdala-insula connectivity and intact ACC-insula connectivity in participants with schizophrenia may indicate compromised capacity to rapidly respond to emotionally salient stimuli in an automatic fashion, but intact capacity to use contextual clues to modulate emotional states. In other words, this potentially indicates an imbalance in the interoceptive inferential process where the bottom-up interoceptive prediction error signals are underweighted compared to the top-down prediction signals. However, it should be acknowledged that it is unclear whether altered white matter integrity indicates altered interoceptive prediction signals, altered interoceptive prediction error signals, or both, as DTI cannot distinguish the direction of axonal fibers.

The lateralized group differences in structural connectivity between amygdala and insula (i.e., decreased connectivity on the left and increased connectivity on the right in SZ) warrants further discussion. My finding that compromised amygdala-insula connectivity in individuals with schizophrenia was specific to the left hemisphere is consistent with a recent activation-likelihood estimation meta-analysis that found disrupted activation only in the left dmIns using different interoceptive probes (e.g., pain, hunger, interoceptive attention) among multiple psychiatric disorders, including schizophrenia (Nord, Lawson, & Dalgleish, 2021), suggesting both functional and structural alterations in the left hemisphere in processing basic interoceptive signals. Conventionally, it was thought that to optimize homeostasis, the right insula was associated with sympathetic activities and energy expenditure, while the left insula was associated with parasympathetic activities and energy enrichment (Craig, 2005; Strigo & Craig, 2016). However, recent studies suggest that this may be too simplistic a view of lateralized

interoception and emotion functions in the brain. When consciously attending to interoceptive signals such as heartbeat and breathing, both sides of insula activated in healthy participants (Failla et al., 2020; Haase et al., 2016; Wiebking et al., 2010) with no difference in level of activation (Haruki & Ogawa, 2021). However, there does seem to be a potential lateralization in interoceptive precision regulation (i.e., assigning more weight to particular interoceptive signals and less weight to "noise") as interoceptive accuracy on a heartbeat counting task was correlated with right insula only (Haruki & Ogawa, 2021). In other words, both sides of insula are involved in processing and interpreting the bodily state, but the right side may have a stronger role in assigning importance to (i.e., weighting) specific interoceptive signals. Therefore, the lateralized group differences in amygdala-insula connections may suggest disruptions in processing bottom-up interoceptive signals in people with schizophrenia, leading to an over reliance on top-down precision regulation as a compensatory response, not unlike the imbalance between amygdala-insula connection and ACC-insula connection discussed above.

At first glance, it is somewhat puzzling that the findings from the corrected total streamline measures (i.e., decreased connectivity in right rACC-dmIns and left vaIns-dpIns connections in SZ and increased connectivity in left amygdala-dmIns connection) were not consistent with those from the diffusivity measures (i.e., decreased connectivity in left amygdala-dmIns and left amygdala-dpIns tracts in SZ and increased connectivity in right amygdala-dmIns tract). One crucial contributing factor to these discrepant findings is that these two measures were quantifying structural connectivity in different ways. Recall that the diffusivity measures were extracted from group tracts thresholded at the 99th percentile of all voxels within the tract, therefore minimizing the effects of individual variability in both the spatial location of the tracts and the number of voxels included in the analysis. In other words, the diffusivity measures

reflect the microstructural white matter integrity of these highly standardized tracts in each individual participant. On the other hand, the measure of total streamlines captures the sum of all streamlines sent from a seed ROI that eventually reaches the target ROI, following the most probable paths (computationally), and contains no information on the spatial location of the streamlines. In other words, an individual could theoretically have a high number of total streamlines due to having more spatially variable tracts alongside the "main" tract (that overlaps with the group standardized tract), rather than having more streamlines going through a centralized main tract. In this case, a higher value on the streamline measure may reflect a more diffuse connection pattern on the individual level, which has no bearing on the diffusivity measure after the spatial standardization procedure. Similarly, higher numbers of streamlines may reflect higher individual variability in the spatial location of the streamlines on the group level. Therefore, one way to interpret the results from the streamline analyses is that participants with schizophrenia had more spatial variability in the left amygdala-dmIns connection than the healthy controls did, and less variability in right rACC-dmIns and left vaIns-dpIns connections.

My finding that emotion recognition ability was correlated with the structural connectivity of pathways within the putative interoception network (specifically, connectivity between ACC and both dmIns and dpIns) in healthy participants is consistent with previous functional neuroimaging literature demonstrating the involvement of ACC and insula in emotion experience and perception (see Lindquist & Barrett, 2012 for review). Moreover, a previous study found that stronger functional connectivity between ACC and dpIns was correlated with better interoceptive ability in healthy participants, supporting the involvement of this connection in interoceptive inference and autonomic regulation (Kleckner et al., 2017). In other words, both the functional and structural connectivity of the ACC-insular connection were associated with

emotional functioning, while the ACC-insular functional connectivity also supported interoception. Therefore, the current study adds to this literature by strengthening the triangulation between emotion, interoception, and ACC-insular connectivity.

Given that perceiving one's own emotional experience and recognizing another individual's emotional state are two distinct processes, it is worth exploring how exactly interoceptive inference can support emotion recognition. Existing literature on facial expression recognition suggests that humans utilize two mechanisms: perceptual and affective (Calvo & Nummenmaa, 2016). The perceptual mechanism relies on referencing the characteristic configurations of facial features associated with different categories of basic emotions (Leppänen & Nelson, 2006). The affective mechanism is the automatic and implicit processing of perceived expressions that is faster than perceptual categorization processes as it only extracts coarse information along the valence and arousal dimensions, rather than deducing a specific emotion label (Calvo & Nummenmaa, 2016; Leppänen & Nelson, 2006). Growing evidence suggests that the affective mechanism is potentially realized through embodied simulation (Folz, Fiacchino, Nikolić, van Steenbergen, & Kret, 2022; Sato, Fujimura, Kochiyama, & Suzuki, 2013). People automatically produce facial expressions that are congruent with the expressions they observe, especially when observing dynamic facial expressions (Hess & Blairy, 2001). The extent of mimicked expressions, indexed by facial muscle activation, are associated with the valence of participants' experienced emotions, which can in turn predict their ability to recognize that emotional expression (Sato et al., 2013). Observing emotional expressions is also associated with automatic physiological changes in the observer, such as increased skin conductance level in response to angry faces and tears and decreased skin temperature in response to sad body

expressions (Folz et al., 2022). Such findings suggest that interoceptive inference may facilitate emotion recognition through embodied simulation of observed emotions (Ondobaka et al., 2017).

It then follows that the weakened relationship between emotion recognition ability and structural connectivity of the interoception network in schizophrenia potentially suggests that people with schizophrenia relied less on the embodied affective mechanism of emotion recognition, which may have contributed to poorer recognition ability. There are consistent findings of facial emotion recognition deficits in schizophrenia, but no consensus on the underlying mechanisms (Gao et al., 2021). On the other hand, there is evidence suggesting potential alterations in facial mimicry, physiological responses to emotional stimuli, as well as recognition of experienced emotions in schizophrenia. Studies in spontaneous facial mimicry suggest that persons with schizophrenia have reduced or altered mimicry response when observing emotional expressions (see Dean, Scott, & Park, 2021 for review). Moreover, reduced mimicry was associated with reduced perceived valence of emotional faces in schizophrenia (Sestito et al., 2013). Another study found that although persons with schizophrenia demonstrated intact facial mimicry, it did not help with their emotion recognition performance, thus suggesting a decoupling between embodied simulation and emotion recognition (Torregrossa et al., 2019). Studies examining physiological responses to emotional images rendered more mixed findings, including greater, same, to less skin conductance reactivity and heart rate changes in persons with schizophrenia compared to healthy participants (see Kring & Moran, 2008 for review; also see S. Park & Kim, 2011; Yee et al., 2010). Lastly, alexithymia (difficulties interpreting one's own emotional states) has been consistently observed in persons with schizophrenia (see O'Driscoll, Laing, & Mason, 2014 for meta-analysis). It has been found that alexithymia is associated with poor recognition of emotional facial expressions, but not

difficulties in recognizing changes in facial features (Cook, Brewer, Shah, & Bird, 2013). In other words, alexithymia may lead to poor emotion recognition through the affective, but not perceptual, mechanism. In sum, alterations in embodied simulation of observed emotions and difficulty interpreting one's own emotional experience (due to altered interoceptive inference) may lead to less reliance on the embodied affective mechanism of emotion recognition in schizophrenia, resulting in poor recognition of facial emotional expressions.

Several limitations need to be considered when interpreting the current findings. First, I would expect that compromised structural connectivity of the putative interoception network should most directly relate to interoceptive functioning; however, I did not have access to measures that assessed interoception directly. Future studies should utilize reliable behavioral paradigms and self-report measures of interoceptive functioning (e.g., Torregrossa et al., 2021) to establish a more direct correlation between brain structures and interoception in persons with schizophrenia. Second, I was not able to rule out potential confounding effects of antipsychotic treatment because current study used a medicated sample. However, the normalized antipsychotic dosages did not correlate with any of the emotional functioning or microstructural measures.

The current study may serve as a springboard for more in-depth mechanistic studies on interoception in schizophrenia. For example, task-based fMRI data may provide an index of interoception more sensitive to temporal changes, and thus may track changes in clinical symptoms more closely. Alternatively, longitudinal studies following people at clinical high risk of psychosis will provide the unique opportunity to assess the baseline functioning of interoception before conversion to full-blown psychosis. This in turn will enable the establishment of a true causal relationship between interoception and clinical symptoms, as well

as the developmental trajectory of such relationship. Experiments manipulating the probabilistic distributions of interoceptive priors and sensory data can help inform where exactly the alterations occur in the interoceptive inference process. Simultaneous collection of data on interoception, emotion experience, and emotion recognition can help establish exactly how faulty interoception may lead to emotion recognition deficits.

In conclusion, I found evidence of altered structural connectivity in a putative interoception network in persons with schizophrenia. Moreover, the structural connectivity of this network in particular was correlated with emotion recognition in healthy control participants, supporting a link between the interoception network and emotional functioning. However, this brain-behavior relationship was much weaker in participants with schizophrenia, suggesting less utilization of this network in emotional functioning. These findings add to our understanding of emotional deficits in schizophrenia and suggest a promising new direction for further research into the role of interoception in illness mechanisms.

APPENDICES

APPENDIX A: Table

Table 1. Demographic and clinical information.

	SZ (N = 35)	HC (N = 36)		
	Mean (SD)	Mean (SD)	Statistic	p
Age (Years)	33.7 (10.4)	33.1 (9.8)	t = 0.25	.80
Sex (Female/Male)	18/17	19/17	χ^2 = 0.013	.91
Education (Years)	14.2 (2.1)	16.1 (1.8)	t = - 4.18	< .001
Parental education	15.3 (2.1)	15.8 (3.1)	t = - 0.83	.41
Childhood SES[a]: medium-high	11	23	χ^2 = 8.08	.04
medium	17	9		
medium-low	5	3		
low	0	1		
WRAT3-R	50.1 (5.4)	51.5 (4.1)	t = -1.23	.22
Race: Asian	0	3	χ^2 = 7.9	.095
Black	15	9		
Native American	0	1		
White	18	22		
Multiracial	2	0		
Unknown	0	1		
Hispanic/Latino (Y/N)	3/32	3/33	χ^2 = .001	.97
ER40 accuracy	30.50 (6.29)	34.42 (2.61)	t = - 3.37	.002
MSCEIT total score	94.10 (19.24)	114.16 (16.99)	t = -4.60	< .001
BDI	15.7 (12.1)	1.8 (2.8)	t = 6.42	< .001
STAI - state anxiety	45.6 (7.8)	37.5 (5.0)	t = 5.12	< .001
SAPS: Total score[b]	16.5 (14.9)	-	-	-
Global summary[b]	4.7 (3.5)	-	-	-
SANS[c]: Total score	20.9 (12.5)	-	-	-
Global summary	6.0 (3.6)	-	-	-
Illness Duration (Years)	13.3 (10.9)	-	-	-
Number of hospitalizations	4.3 (4.9)	-	-	-
BPRS	29.5 (7.5)	-	-	-
Antipsychotics (Y/N)	29/6	-	-	-
CPZ Equivalent (mg)	304.40 (353.15)	-	-	-

Notes: BDI, Beck Depression Inventory; BPRS, Brief Psychiatric Rating Scale; CPZ, chlorpromazine; ER40, Penn Emotion Recognition - 40 Task; HC, healthy control participants; MSCEIT, Mayer-Salovey-Caruso Emotional Intelligence Test; SANS, Scale for the Assessment of Negative Symptoms; SAPS, Scale for the Assessment of Positive Symptoms; STAI, State-

Table 1 (cont'd)
Trait Anxiety Inventory; SZ, participants with schizophrenia; WRAT3-R, Wide Range Achievement Test 3 - Reading.
[a]Childhood SES: (1) High: Family of wealth, education, top-rank social prestige; (2) medium-high: Professional or high-level managerial position; adults hold college or advanced degrees; (3) medium: Small businessmen, white collar and skilled workers, high school grads; (4) medium-low: Semi-skilled workers, laborers, education below secondary level; (5) low: Unskilled and semi-skilled workers, elementary education.
[b]Total score: sum of individual symptom ratings; Global summary: sum of global item ratings.
[c]SANS scores did not include the 2 items on attention due to their poor reliability.

APPENDIX B: Figures

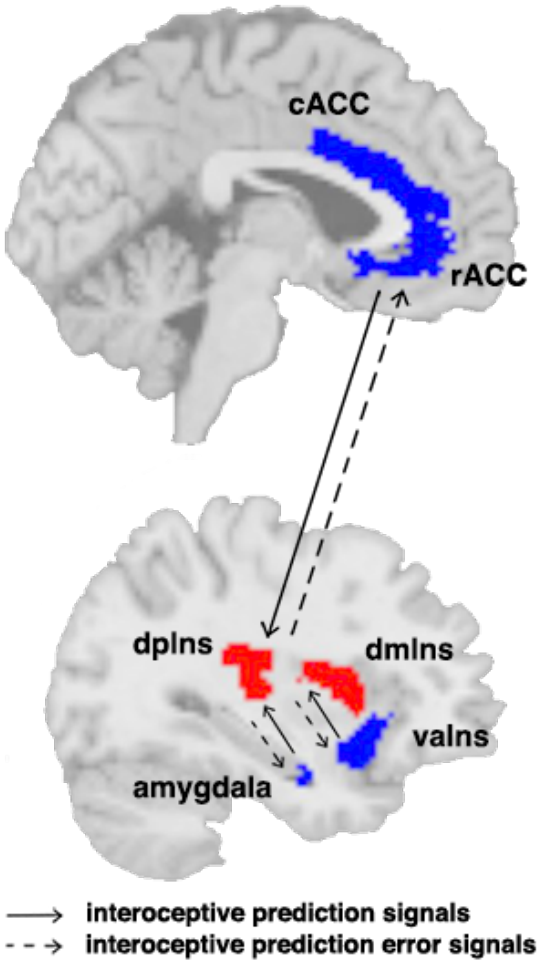

Figure 1. A schematic of the interoceptive network. The red regions are the interoceptive sensory regions (dmIns and dpIns), and the blue regions are the visceromotor control regions (rACC, cACC, amygdala, and vaIns). According to the EPIC model (Barrett & Simmons, 2015), interoceptive prediction signals travel from rACC, cACC, amygdala, and vaIns to dmIns and dpIns, while interoceptive prediction error signals travel the opposite direction. cACC: caudal anterior cingulate cortex; dmIns: dorsal mid insula; dpIns: dorsal posterior insula; rACC: rostral anterior cingulate cortex; vaIns: ventral anterior insula.

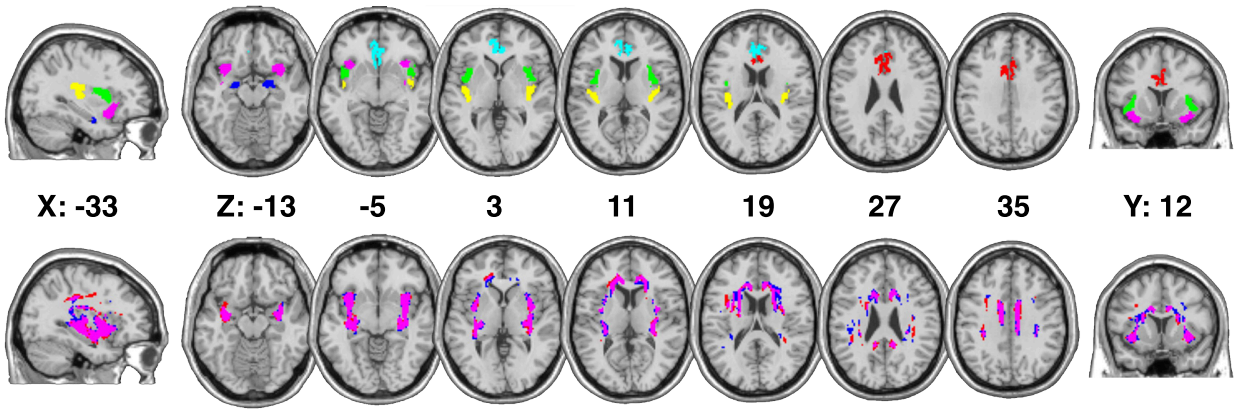

Figure 2. Probabilistic tractography results in both groups. Top panel: ROI masks projected onto a standard-space brain in multi-slice horizontal view; Bottom panel: group-averaged and thresholded white matter tracts in standard space. ROIs are color-coded as follows: amygdala – blue, caudal anterior cingulate cortex – red, rostral anterior cingulate cortex – cyan, ventral anterior insula – pink, dorsal mid insula – green, dorsal posterior insula – yellow. Group-tracts are color-coded as follows: healthy control tracts – blue, schizophrenia participants tracts – red, overlapping tracts – pink. MNI coordinates of each slice were presented in the middle.

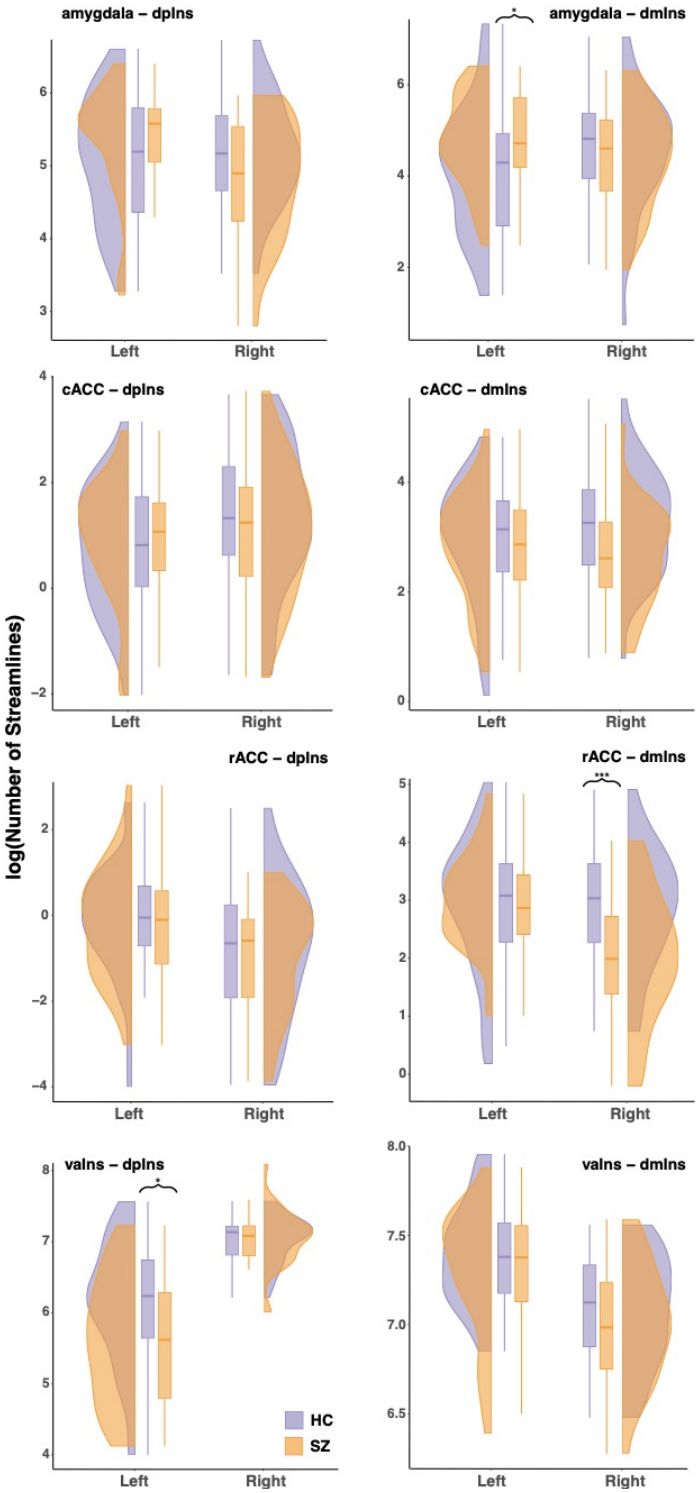

Figure 3. Group differences in the total number of streamlines between ROI pairs by hemisphere. Note that raw measures were used in visualization here for easier interpretation, while corrected and transformed measures were used in the actual group comparison statistical tests. cACC: caudal anterior cingulate cortex; dmIns: dorsal mid insula; dpIns: dorsal posterior insula; rACC: rostral anterior cingulate cortex; vaIns: ventral anterior insula. * $p < .05$, ** $p < .01$, *** $p < .001$.

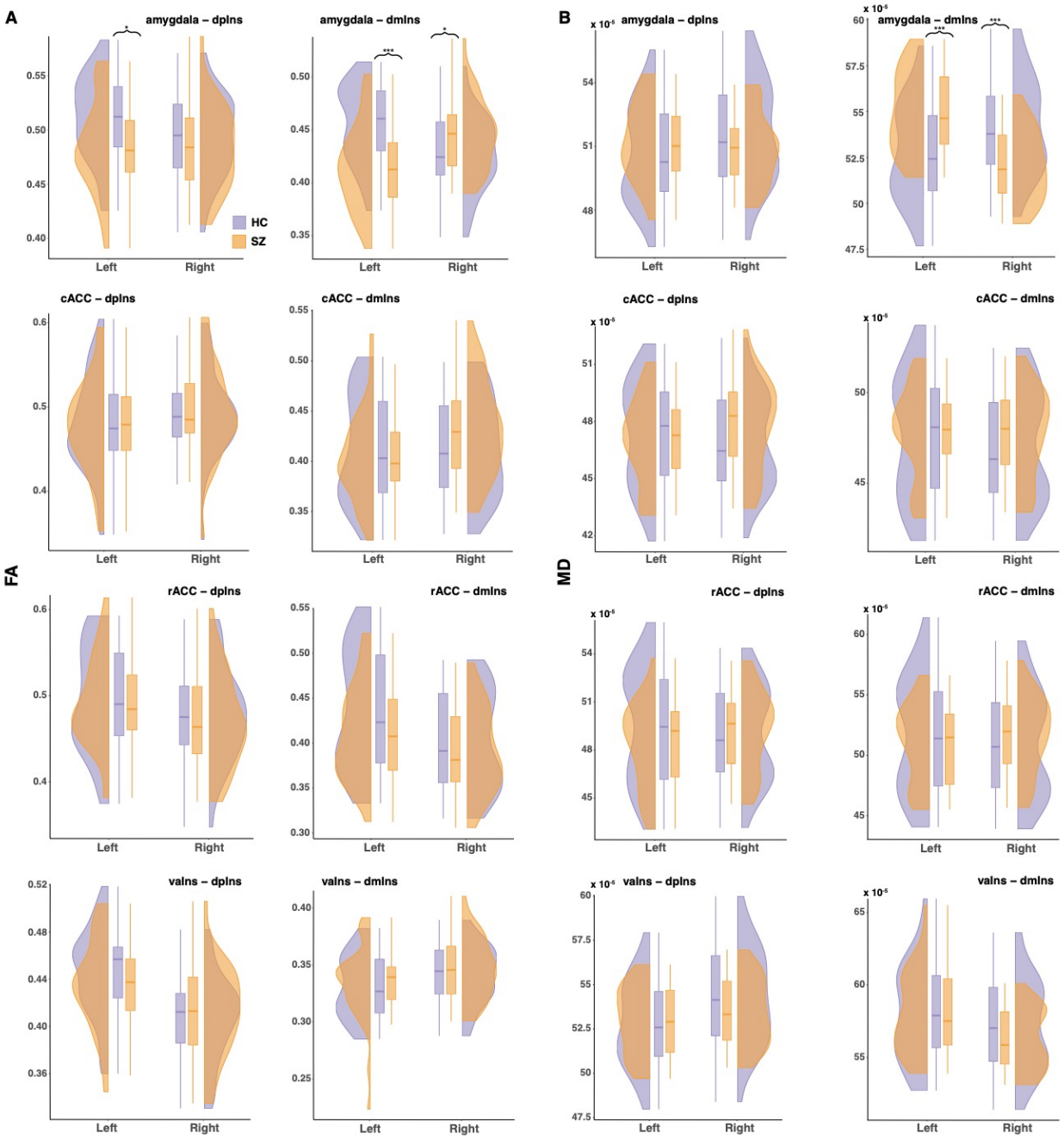

Figure 4. Group differences in the microstructural integrity measures extracted from ROI pairs by hemisphere. A: fractional anisotropy (FA); **B**: mean diffusivity (MD). cACC: caudal anterior cingulate cortex; dmIns: dorsal mid insula; dpIns: dorsal posterior insula; rACC: rostral anterior cingulate cortex; vaIns: ventral anterior insula.
* $p < .05$, ** $p < .01$, *** $p < .001$.

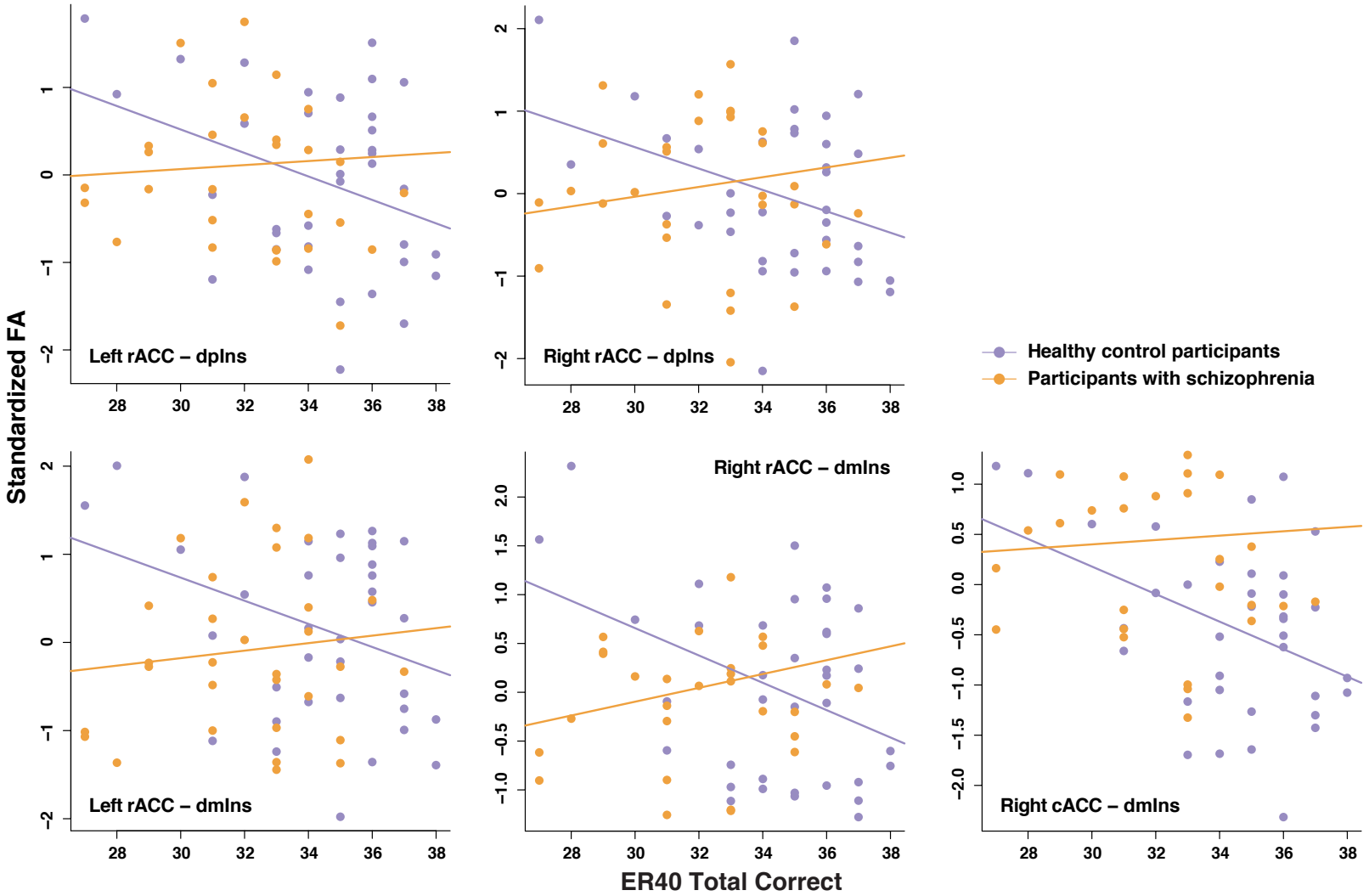

Figure 5. Scatterplots of tract-specific indices of microstructural integrity against emotional functioning. Only ROI pairs with significant group differences in the relationship between standardized residual of tract FA and ER40 performance were included. cACC: caudal anterior cingulate cortex; dmIns: dorsal mid insula; dpIns: dorsal posterior insula; ER40, Penn Emotion Recognition - 40 Task; FA: fractional anisotropy; rACC: rostral anterior cingulate cortex.

APPENDIX C: Supplementary Results

For the corrected total streamline measures, the hemisphere effect was significant in the connections between rACC-dmIns ($F(1,69) = 13.39$, $p < .001$, partial $\eta^2 = 0.16$), rACC-dpIns ($F(1,69) = 11.10$, $p = .001$, partial $\eta^2 = 0.14$), amygdala-dpIns ($F(1,69) = 5.77$, $p = .02$, partial $\eta^2 = 0.08$), vaIns-dmIns ($F(1,69) = 33.67$, $p < .001$, partial $\eta^2 = 0.33$), and vaIns-dpIns ($F(1,69) = 123.64$, $p < .001$, partial $\eta^2 = 0.64$). Post-hoc paired T-tests revealed that the connectivity values were higher in the right than the left vaIns-dpIns connection, but lower in the right hemisphere for all other connections. For the significant group × hemisphere interaction effect in the connection between amygdala and dpIns ($F(1,69) = 11.39$, $p = .001$, partial $\eta^2 = 0.14$), the hemisphere effect was only significant in SZ.

Now for the diffusivity measures, I go through the tracts between each pair of ROIs one by one to discuss results from univariate ANCOVA tests.

For the amygdala-dpIns tract, there was a significant hemisphere effect on FA ($F(1,69) = 12.91$, $p = .001$, partial $\eta^2 = 0.16$), MD ($F(1,69) = 10.38$, $p = .002$, partial $\eta^2 = 0.13$), and RD ($F(1,69) = 15.48$, $p < .001$, partial $\eta^2 = 0.18$), but not on AD ($F(1,69) = 3.09$, $p = .08$, partial $\eta^2 = 0.04$). Post-hoc T-tests revealed that the right hemisphere had lower FA and higher MD and RD than the left hemisphere. There was a significant group × hemisphere interaction effect on MD ($F(1,69) = 39.07$, $p < .001$, partial $\eta^2 = 0.36$) and RD ($F(1,69) = 19.53$, $p < .001$, partial $\eta^2 = 0.22$). Post-hoc T-tests revealed that for both MD and RD, the hemisphere effect was only significant in HC.

For the amygdala-dmIns tract, there was a significant hemisphere effect on MD ($F(1,69) = 80.75$, $p < .001$, partial $\eta^2 = 0.54$), AD ($F(1,69) = 33.48$, $p < .001$, partial $\eta^2 = 0.33$), and RD ($F(1,69) = 22.34$, $p < .001$, partial $\eta^2 = 0.25$), but not on FA ($F(1,69) = 0.13$, $p = .72$, partial $\eta^2 =$

0.002). Post-hoc T-tests revealed that the right hemisphere had lower MD, AD, and RD than the left hemisphere.

For the cACC-dpIns tract, there was a significant hemisphere effect on FA ($F(1,69) = 25.02$, $p < .001$, partial $\eta^2 = 0.27$), MD ($F(1,69) = 4.15$, $p = .046$, partial $\eta^2 = 0.06$), and AD ($F(1,69) = 36.14$, $p < .001$, partial $\eta^2 = 0.34$), but not on RD ($F(1,69) = 2.37$, $p = .13$, partial $\eta^2 = 0.03$). Post-hoc T-tests revealed that the right hemisphere had higher FA, MD, and AD than the left hemisphere. There was a significant group × hemisphere interaction effect on MD ($F(1,69) = 41.93$, $p < .001$, partial $\eta^2 = 0.38$), AD ($F(1,69) = 40.58$, $p < .001$, partial $\eta^2 = 0.37$), and RD ($F(1,69) = 5.21$, $p = .026$, partial $\eta^2 = 0.07$). Post-hoc T-tests revealed that SZ had higher AD than HC, but only in the right hemisphere. HC had higher MD and RD in the left hemisphere than the right, while SZ had the opposite pattern.

For the cACC-dmIns tract, there was a significant hemisphere effect on FA ($F(1,69) = 41.32$, $p < .001$, partial $\eta^2 = 0.38$), MD ($F(1,69) = 9.89$, $p = .002$, partial $\eta^2 = 0.13$), AD ($F(1,69) = 9.69$, $p = .003$, partial $\eta^2 = 0.12$), and RD ($F(1,69) = 51.22$, $p < .001$, partial $\eta^2 = 0.43$). Post-hoc T-tests revealed that the right hemisphere had higher FA and AD and lower MD and RD than the left hemisphere. There was also a significant group × hemisphere interaction effect on FA($F(1,69) = 32.44$, $p < .001$, partial $\eta^2 = 0.32$), AD ($F(1,69) = 27.27$, $p < .001$, partial $\eta^2 = 0.28$), and RD ($F(1,69) = 8.64$, $p = .004$, partial $\eta^2 = 0.11$). Post-hoc T-tests revealed that SZ had higher AD than HC, but only in the right hemisphere. The FA hemisphere effect was only significant in SZ, while the RD hemisphere difference was larger in SZ than in HC.

For the rACC-dpIns tract, there was a significant hemisphere effect on FA ($F(1,69) = 46.42$, $p < .001$, partial $\eta^2 = 0.40$), AD ($F(1,69) = 47.49$, $p < .001$, partial $\eta^2 = 0.41$), and RD ($F(1,69) = 25.46$, $p < .001$, partial $\eta^2 = 0.27$), but not on MD ($F(1,69) = 3.68$, $p = .06$, partial $\eta^2 =$

0.05). Post-hoc T-tests revealed that the right hemisphere had lower FA and AD and higher RD than the left hemisphere. There was also a significant group × hemisphere interaction effect on MD ($F(1,69) = 28.32$, $p < .001$, partial $\eta^2 = 0.29$), AD ($F(1,69) = 44.09$, $p < .001$, partial $\eta^2 = 0.39$), and RD ($F(1,69) = 4.49$, $p = .038$, partial $\eta^2 = 0.06$). Post-hoc T-tests revealed that SZ had lower AD than HC, but only in the left hemisphere. The RD hemisphere effect was only significant in SZ. For MD, the HC had lower diffusivity in the right hemisphere while the SZ had lower diffusivity in the left hemisphere.

For the rACC-dmIns tract, there was a significant hemisphere effect on FA ($F(1,69) = 72.47$, $p < .001$, partial $\eta^2 = 0.51$), AD ($F(1,69) = 81.71$, $p < .001$, partial $\eta^2 = 0.54$), and RD ($F(1,69) = 22.49$, $p < .001$, partial $\eta^2 = 0.25$), but not on MD ($F(1,69) = 0$, $p > .99$, partial $\eta^2 = 0$). Post-hoc T-tests revealed that the right hemisphere had lower FA and AD and higher RD than the left hemisphere. There was also a significant group × hemisphere interaction effect on FA ($F(1,69) = 32.44$, $p < .001$, partial $\eta^2 = 0.32$), MD ($F(1,69) = 19.09$, $p < .001$, partial $\eta^2 = 0.22$), and AD ($F(1,69) = 42.82$, $p < .001$, partial $\eta^2 = 0.38$), but not on RD ($F(1,69) = 2.06$, $p = .16$, partial $\eta^2 = 0.03$). Post-hoc T-tests revealed that SZ had lower AD than HC, but only in the left hemisphere. The FA hemisphere difference was larger in HC. For MD, the HC had lower diffusivity in the right hemisphere while the SZ had lower diffusivity in the left hemisphere.

For the vaIns-dpIns tract, there was a significant hemisphere effect on FA ($F(1,69) = 125.52$, $p < .001$, partial $\eta^2 = 0.65$), MD ($F(1,69) = 76.19$, $p < .001$, partial $\eta^2 = 0.53$), AD ($F(1,69) = 34.19$, $p < .001$, partial $\eta^2 = 0.33$), and RD ($F(1,69) = 115.62$, $p < .001$, partial $\eta^2 = 0.63$). Post-hoc T-tests revealed that the right hemisphere had lower FA and AD and higher MD and RD than the left hemisphere. There was also a significant group × hemisphere interaction effect on FA ($F(1,69) = 7.52$, $p = .008$, partial $\eta^2 = 0.10$), MD ($F(1,69) = 17.57$, $p < .001$, partial

η^2 = 0.20), and RD (F(1,69) = 12.15, p = .001, partial η^2 = 0.15), but not on AD (F(1,69) = 1.14, p = .29, partial η^2 = 0.02). Post-hoc T-tests revealed that the FA and RD hemisphere differences were larger in HC, while the MD hemisphere difference was larger in SZ.

For the vaIns-dmIns tract, there was a significant hemisphere effect on FA (F(1,69) = 21.19, p < .001, partial η^2 = 0.24), MD (F(1,69) = 108.93, p < .001, partial η^2 = 0.61), AD (F(1,69) = 55.23, p < .001, partial η^2 = 0.45), and RD (F(1,69) = 64.92, p < .001, partial η^2 = 0.49). Post-hoc T-tests revealed that the right hemisphere had higher FA and lower MD, AD, and RD than the left hemisphere. There was also a significant group × hemisphere interaction effect on MD (F(1,69) = 13.53, p < .001, partial η^2 = 0.16), AD (F(1,69) = 16.81, p < .001, partial η^2 = 0.20), and RD (F(1,69) = 4.91, p = .03, partial η^2 = 0.07). Post-hoc T-tests revealed that the MD, AD, and RD hemisphere differences were larger in SZ.

Table S1. Percent of outlier slices and average head translations, rotations, and total displacements (in raw and absolute values).

	SZ (N = 35)		HC (N = 36)			
Metrics	Mean	SD	Mean	SD	t	p
Percent of outlier slices	0.40	0.24	0.39	0.25	-0.17	.86
Mean x translation	0.009	0.23	-0.03	0.21	-0.81	.42
Mean x translation (absolute value)	0.16	0.16	0.16	0.13	0.13	.90
Mean y translation	0.57	0.31	0.57	0.20	-0.01	.99
Mean y translation (absolute value)	0.57	0.29	0.57	0.20	-0.13	.90
Mean z translation	-0.19	0.40	-0.23	0.38	-0.40	.69
Mean z translation (absolute value)	0.33	0.29	0.3	0.32	-0.40	.69
Mean x rotation	0.20	0.37	0.24	0.33	0.48	.63
Mean x rotation (absolute value)	0.30	0.29	0.28	0.28	-0.25	.80
Mean y rotation	0.07	0.28	0.01	0.19	-1.04	.30
Mean y rotation (absolute value)	0.21	0.19	0.15	0.11	-1.62	.11
Mean z rotation	0.02	0.18	-0.002	0.16	-0.55	.58
Mean z rotation (absolute value)	0.13	0.13	0.12	0.11	-0.30	.77
Mean absolute total displacement	0.61	0.34	0.55	0.33	-0.83	.41
Mean relative total displacement	0.20	0.07	0.19	0.07	-0.55	.58

Notes: HC, healthy control participants; SZ, participants with schizophrenia.

Table S2. Linear regression coefficients estimating effects of diagnostic group and MSCEIT total score on standardized FA from each tract within the putative interoception network.

Tract	Variable	*b*	*t*(65)	*p*
amygdala-dpIns	Group	-0.61	-2.24	.03
	MSCEIT	-0.01	-1.17	.25
	Group × MSCEIT	0.007	0.50	.62
Left amygdala-dmIns	Group	-1.13	-4.84	< .001
	MSCEIT	-0.01	-1.38	.17
	Group × MSCEIT	0.01	1.23	.22
Right amygdala-dmIns	Group	0.73	2.93	.005
	MSCEIT	-0.02	-1.94	.06
	Group × MSCEIT	0.02	1.67	.10
Left cACC-dpIns	Group	0.16	0.57	.57
	MSCEIT	0.003	0.32	.75
	Group × MSCEIT	-0.003	-0.23	.82
Right cACC-dpIns	Group	0.32	1.15	.26
	MSCEIT	-0.008	-0.83	.41
	Group × MSCEIT	0.02	1.20	.24
Left cACC-dmIns	Group	-0.10	-0.37	.71
	MSCEIT	0.001	0.14	.89
	Group × MSCEIT	-0.01	-0.74	.46
Right cACC-dmIns	Group	0.81	3.22	.002
	MSCEIT	-0.004	-0.49	.63
	Group × MSCEIT	0.008	0.62	.54
Left rACC-dpIns	Group	0.13	0.46	.65
	MSCEIT	-0.00008	-0.01	.99
	Group × MSCEIT	0.003	0.21	.84
Right rACC-dpIns	Group	0.02	0.08	.94
	MSCEIT	-0.009	-0.90	.37
	Group × MSCEIT	0.02	1.68	.10
Left rACC-dmIns	Group	-0.38	-1.39	.17
	MSCEIT	0.003	0.32	.75
	Group × MSCEIT	-0.007	-0.55	.59
Right rACC-dmIns	Group	-0.06	-0.21	.83
	MSCEIT	-0.002	-0.22	.83
	Group × MSCEIT	0.01	0.74	.46
Left vaIns-dpIns	Group	-0.23	-0.82	.41
	MSCEIT	-0.01	-1.20	.24

Table S2 (cont'd)

	Group × MSCEIT	0.01	0.78	.44
Right vaIns-dpIns	Group	0.18	0.66	.51
	MSCEIT	-0.01	-1.26	.21
	Group × MSCEIT	0.007	0.50	.62
Left vaIns-dmIns	Group	0.37	1.38	.17
	MSCEIT	-0.01	-1.21	.23
	Group × MSCEIT	0.02	1.50	.14
Right vaIns-dmIns	Group	0.17	0.64	.53
	MSCEIT	-0.02	-2.28	.03
	Group × MSCEIT	0.02	1.22	.23

Notes: HC is the implicit reference group. cACC: caudal anterior cingulate cortex; dmIns: dorsal mid insula; dpIns: dorsal posterior insula; MSCEIT, Mayer-Salovey-Caruso Emotional Intelligence Test; rACC: rostral anterior cingulate cortex.

Table S3. Linear regression coefficients estimating effects of diagnostic group and ER40 accuracy score on standardized FA from each tract within the putative interoception network.

Tract	Variable	*b*	*t*(66)	*p*
amygdala-dpIns	Group	-0.53	-1.97	.05
	ER40	-0.07	-1.05	.30
	Group × ER40	0.08	1.12	.27
Left amygdala-dmIns	Group	-1.16	-5.07	< .001
	ER40	-0.08	-1.42	.16
	Group × ER40	0.09	1.50	.14
Right amygdala-dmIns	Group	0.65	2.66	.01
	ER40	-0.11	-1.96	.05
	Group × ER40	0.11	1.74	.09
Left cACC-dpIns	Group	0.007	0.03	.98
	ER40	-0.10	-1.52	.13
	Group × ER40	0.11	1.63	.11
Right cACC-dpIns	Group	0.20	0.74	.46
	ER40	-0.09	-1.48	.14
	Group × ER40	0.12	1.75	.09
Left cACC-dmIns	Group	-0.19	-0.69	.49
	ER40	-0.12	-1.90	.06
	Group × ER40	0.14	2.02	.048
Right cACC-dmIns	Group	0.62	2.60	.01
	ER40	-0.14	-2.44	.02
	Group × ER40	0.16	2.60	.01
Left rACC-dpIns	Group	-0.06	-0.22	.83
	ER40	-0.13	-2.11	.04
	Group × ER40	0.16	2.27	.03
Right rACC-dpIns	Group	-0.13	-0.49	.63
	ER40	-0.13	-2.10	.04
	Group × ER40	0.19	2.81	.007
Left rACC-dmIns	Group	-0.48	-1.81	.08
	ER40	-0.13	-2.11	.04
	Group × ER40	0.17	2.57	.01
Right rACC-dmIns	Group	-0.22	-0.88	.38
	ER40	-0.14	-2.33	.02
	Group × ER40	0.21	3.22	.002
Left vaIns-dpIns	Group	-0.14	-0.51	.61
	ER40	-0.04	-0.58	.56

Table S3 (cont'd)

	Group × ER40	0.04	0.56	.58
Right vaIns-dpIns	Group	0.33	1.20	.23
	ER40	-0.05	-0.82	.41
	Group × ER40	0.07	1.07	.29
Left vaIns-dmIns	Group	0.32	1.21	.23
	ER40	-0.04	-0.62	.54
	Group × ER40	0.04	0.58	.56
Right vaIns-dmIns	Group	0.35	1.29	.20
	ER40	-0.04	-0.62	.54
	Group × ER40	0.03	0.48	.63

Notes: HC is the implicit reference group. cACC: caudal anterior cingulate cortex; dmIns: dorsal mid insula; dpIns: dorsal posterior insula; ER40, Penn Emotion Recognition - 40 Task; rACC: rostral anterior cingulate cortex.

Table S4. Spearman's rank correlation between clinical symptom scores and standardized FA from the tracts that differed in connectivity between the two groups.

		SAPS				SANS			
		Total score		Global summary		Total score		Global summary	
		r_s	p	r_s	p	r_s	p	r_s	p
amygdala - dpIns		0.13	.47	0.13	.47	0.02	.91	0.05	.78
amygdala - dmIns	left	0.09	.62	0.02	.90	-0.19	.28	-0.22	.20
	right	0.09	.62	0.10	.57	0.01	.95	0.01	.96

Notes: Global summary: sum of global item ratings; SANS, Scale for the Assessment of Negative Symptoms; SAPS, Scale for the Assessment of Positive Symptoms; Total score: sum of individual symptom ratings.

REFERENCES

REFERENCES

Abe, O., Aoki, S., Hayashi, N., Yamada, H., Kunimatsu, A., Mori, H., … Ohtomo, K. (2002). Normal aging in the central nervous system: Quantitative MR diffusion-tensor analysis. *Neurobiology of Aging*, *23*(3), 433–441. https://doi.org/10.1016/S0197-4580(01)00318-9

Alexander, A. L., Lee, J. E., Lazar, M., & Field, A. S. (2007). Diffusion tensor imaging of the brain. *Neurotherapeutics*, *4*(3), 316–329. https://doi.org/10.1016/j.nurt.2007.05.011

Amodio, A., Quarantelli, M., Mucci, A., Prinster, A., Soricelli, A., Vignapiano, A., … Galderisi, S. (2018). Avolition-Apathy and White Matter Connectivity in Schizophrenia: Reduced Fractional Anisotropy Between Amygdala and Insular Cortex. *Clinical EEG and Neuroscience*, *49*(1), 55–65. https://doi.org/10.1177/1550059417745934

Andreasen, N. C. (1984a). *Scale for the Assessment of Negative Symptoms (SANS)*. Iowa City, IA: University of Iowa.

Andreasen, N. C. (1984b). *Scale for the Assessment of Positive Symptoms (SAPS).* Iowa City, IA: University of Iowa.

Andreasen, N. C., Pressler, M., Nopoulos, P., Miller, D., & Ho, B.-C. (2010). Antipsychotic Dose Equivalents and Dose-Years: A Standardized Method for Comparing Exposure to Different Drugs. *Biological Psychiatry*, *67*(3), 255–262. https://doi.org/10.1016/j.biopsych.2009.08.040

Ardizzi, M., Ambrosecchia, M., Buratta, L., Ferri, F., Peciccia, M., Donnari, S., … Gallese, V. (2016). Interoception and Positive Symptoms in Schizophrenia. *Frontiers in Human Neuroscience*, *10*, 379. https://doi.org/10.3389/fnhum.2016.00379

Barrett, L. F. (2017). The theory of constructed emotion: an active inference account of interoception and categorization. *Social Cognitive and Affective Neuroscience*, *12*(1), 1–23. https://doi.org/10.1093/scan/nsw154

Barrett, L. F., & Simmons, W. K. (2015). Interoceptive predictions in the brain. *Nature Reviews Neuroscience*, *16*(7), 419–429. https://doi.org/10.1038/nrn3950

Behrens, T. E. J., Berg, H. J., Jbabdi, S., Rushworth, M. F. S., & Woolrich, M. W. (2007). Probabilistic diffusion tractography with multiple fibre orientations: What can we gain? *NeuroImage*, *34*(1), 144–155. https://doi.org/10.1016/j.neuroimage.2006.09.018

Behrens, T. E. J., Woolrich, M. W., Jenkinson, M., Johansen-Berg, H., Nunes, R. G., Clare, S., … Smith, S. M. (2003). Characterization and propagation of uncertainty in diffusion-weighted MR imaging. *Magnetic Resonance in Medicine*, *50*(5), 1077–1088. https://doi.org/10.1002/mrm.10609

Bennett, I. J., Madden, D. J., Vaidya, C. J., Howard, D. V., & Howard, J. H. (2010). Age-related differences in multiple measures of white matter integrity: A diffusion tensor imaging study of healthy aging. *Human Brain Mapping*, *31*(3), 378–390. https://doi.org/10.1002/hbm.20872

Bersani, F. S., Minichino, A., Fojanesi, M., Gallo, M., Maglio, G., Valeriani, G., … Fitzgerald, P. B. (2014). Cingulate Cortex in Schizophrenia: Its relation with negative symptoms and psychotic onset. A review study. *European Review for Medical and Pharmacological Sciences*, *18*(22), 3354–3367. https://doi.org/10.1111/j.1601-5215.2011.00640.x

Brener, J., & Ring, C. (2016). Towards a psychophysics of interoceptive processes: the measurement of heartbeat detection. *Philosophical Transactions of the Royal Society B: Biological Sciences*, *371*(1708), 20160015. https://doi.org/10.1098/rstb.2016.0015

Calvo, M. G., & Nummenmaa, L. (2016). Perceptual and affective mechanisms in facial expression recognition: An integrative review. *Cognition and Emotion*, *30*(6), 1081–1106. https://doi.org/10.1080/02699931.2015.1049124

Chong, T. W. ., & Castle, D. J. (2004). Layer upon layer: thermoregulation in schizophrenia. *Schizophrenia Research*, *69*(2–3), 149–157. https://doi.org/10.1016/S0920-9964(03)00222-6

Clamor, A., Lincoln, T. M., Thayer, J. F., & Koenig, J. (2016). Resting vagal activity in schizophrenia: Meta-analysis of heart rate variability as a potential endophenotype. *British Journal of Psychiatry*, *208*(1), 9–16. https://doi.org/10.1192/bjp.bp.114.160762

Cohen, A. L., Fair, D. A., Dosenbach, N. U. F., Miezin, F. M., Dierker, D., Van Essen, D. C., … Petersen, S. E. (2008). Defining functional areas in individual human brains using resting functional connectivity MRI. *NeuroImage*, *41*(1), 45–57. https://doi.org/10.1016/j.neuroimage.2008.01.066

Cook, R., Brewer, R., Shah, P., & Bird, G. (2013). Alexithymia, Not Autism, Predicts Poor Recognition of Emotional Facial Expressions. *Psychological Science*, *24*(5), 723–732. https://doi.org/10.1177/0956797612463582

Craig, A. D. (Bud). (2005). Forebrain emotional asymmetry: a neuroanatomical basis? *Trends in Cognitive Sciences*, *9*(12), 566–571. https://doi.org/10.1016/j.tics.2005.10.005

Critchley, H. D., Ewing, D. L., van Praag, C. G., Habash-Bailey, H., Eccles, J. A., Meeten, F., & Garfinkel, S. N. (2019). Transdiagnostic expression of interoceptive abnormalities in psychiatric conditions. *MedRxiv*, 19012393. https://doi.org/https://doi.org/10.1101/19012393

Danivas, V., & Venkatasubramanian, G. (2013). Current perspectives on chlorpromazine equivalents: Comparing apples and oranges! *Indian Journal of Psychiatry*, *55*(2), 207–208. https://doi.org/10.4103/0019-5545.111475

Davis, K. L., Stewart, D. G., Friedman, J. I., Buchsbaum, M., Harvey, P. D., Hof, P. R., … Haroutunian, V. (2003). White Matter Changes in Schizophrenia. *Archives of General Psychiatry*, *60*(5), 443–456. https://doi.org/10.1001/archpsyc.60.5.443

Dean, D. J., Scott, J., & Park, S. (2021). Interpersonal Coordination in Schizophrenia: A Scoping Review of the Literature. *Schizophrenia Bulletin*, *47*(6), 1544–1556. https://doi.org/10.1093/schbul/sbab072

Failla, M. D., Bryant, L. K., Heflin, B. H., Mash, L. E., Schauder, K., Davis, S., … Cascio, C. J. (2020). Neural Correlates of Cardiac Interoceptive Focus Across Development: Implications for Social Symptoms in Autism Spectrum Disorder. *Autism Research*, *13*(6), 908–920. https://doi.org/10.1002/aur.2289

Fan, L., Li, H., Zhuo, J., Zhang, Y., Wang, J., Chen, L., … Jiang, T. (2016). The Human Brainnetome Atlas: A New Brain Atlas Based on Connectional Architecture. *Cerebral Cortex*, *26*(8), 3508–3526. https://doi.org/10.1093/cercor/bhw157

Feldman, H. M., Yeatman, J. D., Lee, E. S., Barde, L. H. F., & Gaman-Bean, S. (2010). Diffusion Tensor Imaging: A Review for Pediatric Researchers and Clinicians. *Journal of Developmental & Behavioral Pediatrics*, *31*(4), 346–356. https://doi.org/10.1097/DBP.0b013e3181dcaa8b

Folz, J., Fiacchino, D., Nikolić, M., van Steenbergen, H., & Kret, M. E. (2022). Reading Your Emotions in My Physiology? Reliable Emotion Interpretations in Absence of a Robust Physiological Resonance. *Affective Science*. https://doi.org/10.1007/s42761-021-00083-5

Gao, Z., Zhao, W., Liu, S., Liu, Z., Yang, C., & Xu, Y. (2021). Facial Emotion Recognition in Schizophrenia. *Frontiers in Psychiatry*, *12*(May), 1–10. https://doi.org/10.3389/fpsyt.2021.633717

Gorgolewski, K. J., Auer, T., Calhoun, V. D., Craddock, R. C., Das, S., Duff, E. P., … Poldrack, R. A. (2016). The brain imaging data structure, a format for organizing and describing outputs of neuroimaging experiments. *Scientific Data*, *3*(1), 160044. https://doi.org/10.1038/sdata.2016.44

Goswami, S., Beniwal, R. P., Kumar, M., Bhatia, T., Gur, R. E., Gur, R. C., … Deshpande, S. N. (2020). A preliminary study to investigate resting state fMRI as a potential group differentiator for schizophrenia. *Asian Journal of Psychiatry*, *52*, 102095. https://doi.org/10.1016/j.ajp.2020.102095

Greve, D. N., & Fischl, B. (2009). Accurate and robust brain image alignment using boundary-based registration. *NeuroImage*, *48*(1), 63–72. https://doi.org/10.1016/j.neuroimage.2009.06.060

Gu, X., & FitzGerald, T. H. B. (2014). Interoceptive inference: homeostasis and decision-making. *Trends in Cognitive Sciences*, *18*(6), 269–270.

https://doi.org/10.1016/j.tics.2014.02.001

Gur, R. C., Sara, R., Hagendoorn, M., Marom, O., Hughett, P., Macy, L., … Gur, R. E. (2002). A method for obtaining 3-dimensional facial expressions and its standardization for use in neurocognitive studies. *Journal of Neuroscience Methods*, *115*(2), 137–143. https://doi.org/10.1016/S0165-0270(02)00006-7

Haase, L., Stewart, J. L., Youssef, B., May, A. C., Isakovic, S., Simmons, A. N., … Paulus, M. P. (2016). When the brain does not adequately feel the body: Links between low resilience and interoception. *Biological Psychology*, *113*, 37–45. https://doi.org/10.1016/j.biopsycho.2015.11.004

Haruki, Y., & Ogawa, K. (2021). Role of anatomical insular subdivisions in interoception: Interoceptive attention and accuracy have dissociable substrates. *European Journal of Neuroscience*, *53*(8), 2669–2680. https://doi.org/10.1111/ejn.15157

Hess, U., & Blairy, S. (2001). Facial mimicry and emotional contagion to dynamic emotional facial expressions and their influence on decoding accuracy. *International Journal of Psychophysiology*, *40*(2), 129–141. https://doi.org/10.1016/S0167-8760(00)00161-6

Hiser, J., & Koenigs, M. (2018). The Multifaceted Role of the Ventromedial Prefrontal Cortex in Emotion, Decision Making, Social Cognition, and Psychopathology. *Biological Psychiatry*, *83*(8), 638–647. https://doi.org/10.1016/j.biopsych.2017.10.030

Jaaskelainen, E., Juola, P., Hirvonen, N., McGrath, J. J., Saha, S., Isohanni, M., … Miettunen, J. (2013). A Systematic Review and Meta-Analysis of Recovery in Schizophrenia. *Schizophrenia Bulletin*, *39*(6), 1296–1306. https://doi.org/10.1093/schbul/sbs130

Kleckner, I. R., Zhang, J., Touroutoglou, A., Chanes, L., Xia, C., Simmons, W. K., … Feldman Barrett, L. (2017). Evidence for a large-scale brain system supporting allostasis and interoception in humans. *Nature Human Behaviour*, *1*(5), 0069. https://doi.org/10.1038/s41562-017-0069

Koreki, A., Funayama, M., Terasawa, Y., Onaya, M., & Mimura, M. (2020). Aberrant interoceptive accuracy in patients with schizophrenia performing a heartbeat counting task. *Schizophrenia Bulletin Open*. https://doi.org/10.1093/schizbullopen/sgaa067

Kring, A. M., & Moran, E. K. (2008). Emotional Response Deficits in Schizophrenia: Insights From Affective Science. *Schizophrenia Bulletin*, *34*(5), 819–834. https://doi.org/10.1093/schbul/sbn071

Landman, B. A., Bogovic, J. A., Wan, H., ElShahaby, F. E. Z., Bazin, P.-L., & Prince, J. L. (2012). Resolution of crossing fibers with constrained compressed sensing using diffusion tensor MRI. *NeuroImage*, *59*(3), 2175–2186. https://doi.org/10.1016/j.neuroimage.2011.10.011

Laursen, T. M., Nordentoft, M., & Mortensen, P. B. (2014). Excess Early Mortality in Schizophrenia. *Annual Review of Clinical Psychology*, *10*(1), 425–448. https://doi.org/10.1146/annurev-clinpsy-032813-153657

Leppänen, J. M., & Nelson, C. A. (2006). The development and neural bases of facial emotion recognition. In *Advances in Child Development and Behavior* (Vol. 34, pp. 207–246). https://doi.org/10.1016/S0065-2407(06)80008-X

Lindquist, K. A., & Barrett, L. F. (2012). A functional architecture of the human brain: Emerging insights from the science of emotion. *Trends in Cognitive Sciences*, *16*(11), 533–540. https://doi.org/10.1016/j.tics.2012.09.005

Maher, B. (2005). Delusional thinking and cognitive disorder. *Integrative Physiological & Behavioral Science*, *40*(3), 136–146. https://doi.org/10.1007/BF03159710

Makowski, D., Sperduti, M., Blondé, P., Nicolas, S., & Piolino, P. (2020). The heart of cognitive control: Cardiac phase modulates processing speed and inhibition. *Psychophysiology*, *57*(3), 1–11. https://doi.org/10.1111/psyp.13490

Mayer, J. D., Salovey, P., & Caruso, D. R. (1999). *Mayer-Salovey-Caruso Emotional Intelligence Test.* North Tonawanda, NY: Multi-Health Systems Inc.

Mori, S., & van Zijl, P. C. M. (2002). Fiber tracking: principles and strategies - a technical review. *NMR in Biomedicine*, *15*(7–8), 468–480. https://doi.org/10.1002/nbm.781

Mori, S., & Zhang, J. (2006). Principles of Diffusion Tensor Imaging and Its Applications to Basic Neuroscience Research. *Neuron*, *51*(5), 527–539. https://doi.org/10.1016/j.neuron.2006.08.012

Nord, C. L., Lawson, R. P., & Dalgleish, T. (2021). Disrupted Dorsal Mid-Insula Activation During Interoception Across Psychiatric Disorders. *American Journal of Psychiatry*, *178*(8), 761–770. https://doi.org/10.1176/appi.ajp.2020.20091340

O'Driscoll, C., Laing, J., & Mason, O. (2014). Cognitive emotion regulation strategies, alexithymia and dissociation in schizophrenia, a review and meta-analysis. *Clinical Psychology Review*, *34*(6), 482–495. https://doi.org/10.1016/j.cpr.2014.07.002

Ondobaka, S., Kilner, J., & Friston, K. (2017). The role of interoceptive inference in theory of mind. *Brain and Cognition*, *112*, 64–68. https://doi.org/10.1016/j.bandc.2015.08.002

Overall, J. E., & Gorham, D. R. (1962). The Brief Psychiatric Rating Scale. *Psychological Reports*, *10*(3), 799–812. https://doi.org/10.2466/pr0.1962.10.3.799

Park, S., & Kim, K. (2011). Physiological Reactivity and Facial Expression to Emotion-Inducing Films in Patients With Schizophrenia. *Archives of Psychiatric Nursing*, *25*(6), e37–e47. https://doi.org/10.1016/j.apnu.2011.08.001

Pramme, L., Larra, M. F., Schächinger, H., & Frings, C. (2014). Cardiac cycle time effects on mask inhibition. *Biological Psychology*, *100*, 115–121. https://doi.org/10.1016/j.biopsycho.2014.05.008

Pramme, L., Larra, M. F., Schächinger, H., & Frings, C. (2016). Cardiac cycle time effects on selection efficiency in vision. *Psychophysiology*, *53*(11), 1702–1711. https://doi.org/10.1111/psyp.12728

Ring, C., & Brener, J. (2018). Heartbeat counting is unrelated to heartbeat detection: A comparison of methods to quantify interoception. *Psychophysiology*, *55*(9), e13084. https://doi.org/10.1111/psyp.13084

Rothe, P. H., Heres, S., & Leucht, S. (2018). Dose equivalents for second generation long-acting injectable antipsychotics: The minimum effective dose method. *Schizophrenia Research*, *193*, 23–28. https://doi.org/10.1016/j.schres.2017.07.033

Sato, W., Fujimura, T., Kochiyama, T., & Suzuki, N. (2013). Relationships among Facial Mimicry, Emotional Experience, and Emotion Recognition. *PLoS ONE*, *8*(3), e57889. https://doi.org/10.1371/journal.pone.0057889

Schulkin, J., & Sterling, P. (2019). Allostasis: A Brain-Centered, Predictive Mode of Physiological Regulation. *Trends in Neurosciences*. https://doi.org/10.1016/j.tins.2019.07.010

Seamans, J. K., & Floresco, S. B. (2022). Event-based control of autonomic and emotional states by the anterior cingulate cortex. *Neuroscience & Biobehavioral Reviews*, *133*(December 2021), 104503. https://doi.org/10.1016/j.neubiorev.2021.12.026

Sestito, M., Alessandra Umiltà, M., De Paola, G., Fortunati, R., Raballo, A., Leuci, E., … Gallese, V. (2013). Facial reactions in response to dynamic emotional stimuli in different modalities in patients suffering from schizophrenia: A behavioral and EMG study. *Frontiers in Human Neuroscience*, *7*(JUN), 1–12. https://doi.org/10.3389/fnhum.2013.00368

Seth, A. K. (2013). Interoceptive inference, emotion, and the embodied self. *Trends in Cognitive Sciences*, *17*(11), 565–573. https://doi.org/10.1016/j.tics.2013.09.007

Seth, A. K. (2015). The Cybernetic Bayesian Brain: From Interoceptive Inference to Sensorimotor Contingencies. In T. K. Metzinger & J. M. Windt (Eds.), *Open MIND*. Frankfurt am Main: MIND Group. https://doi.org/10.15502/9783958570108

Seth, A. K., & Friston, K. J. (2016). Active interoceptive inference and the emotional brain. *Philosophical Transactions of the Royal Society B: Biological Sciences*, *371*(1708), 20160007. https://doi.org/10.1098/rstb.2016.0007

Seth, A. K., Suzuki, K., & Critchley, H. D. (2012). An Interoceptive Predictive Coding Model of Conscious Presence. *Frontiers in Psychology*, *2*. https://doi.org/10.3389/fpsyg.2011.00395

Sher, L., & Kahn, R. S. (2019). Suicide in Schizophrenia: An Educational Overview. *Medicina*, *55*(7), 361. https://doi.org/10.3390/medicina55070361

Silverstein, S. M. (2016). Visual Perception Disturbances in Schizophrenia: A Unified Model. In W. Spaulding (Ed.), *The Neuropsychopathology of Schizophrenia. Nebraska Symposium on Motivation* (Vol. 63, pp. 77–132). Springer, Cham. https://doi.org/10.1007/978-3-319-30596-7_4

Šimić, G., Tkalčić, M., Vukić, V., Mulc, D., Španić, E., Šagud, M., … R. Hof, P. (2021). Understanding Emotions: Origins and Roles of the Amygdala. *Biomolecules*, *11*(6), 823. https://doi.org/10.3390/biom11060823

Smith, R., Thayer, J. F., Khalsa, S. S., & Lane, R. D. (2017). The hierarchical basis of neurovisceral integration. *Neuroscience & Biobehavioral Reviews*, *75*, 274–296. https://doi.org/10.1016/j.neubiorev.2017.02.003

Snook, L., Plewes, C., & Beaulieu, C. (2007). Voxel based versus region of interest analysis in diffusion tensor imaging of neurodevelopment. *NeuroImage*, *34*(1), 243–252. https://doi.org/10.1016/j.neuroimage.2006.07.021

Song, S.-K., Sun, S.-W., Ju, W.-K., Lin, S.-J., Cross, A. H., & Neufeld, A. H. (2003). Diffusion tensor imaging detects and differentiates axon and myelin degeneration in mouse optic nerve after retinal ischemia. *NeuroImage*, *20*(3), 1714–1722. https://doi.org/10.1016/j.neuroimage.2003.07.005

Song, S.-K., Sun, S.-W., Ramsbottom, M. J., Chang, C., Russell, J., & Cross, A. H. (2002). Dysmyelination Revealed through MRI as Increased Radial (but Unchanged Axial) Diffusion of Water. *NeuroImage*, *17*(3), 1429–1436. https://doi.org/10.1006/nimg.2002.1267

Stephan, K. E., Manjaly, Z. M., Mathys, C. D., Weber, L. A. E., Paliwal, S., Gard, T., … Petzschner, F. H. (2016). Allostatic Self-efficacy: A Metacognitive Theory of Dyshomeostasis-Induced Fatigue and Depression. *Frontiers in Human Neuroscience*, *10*, 550. https://doi.org/10.3389/fnhum.2016.00550

Sterling, P. (2012). Allostasis: A model of predictive regulation. *Physiology & Behavior*, *106*(1), 5–15. https://doi.org/10.1016/j.physbeh.2011.06.004

Strigo, I. A., & Craig, A. D. (Bud). (2016). Interoception, homeostatic emotions and sympathovagal balance. *Philosophical Transactions of the Royal Society B: Biological Sciences*, *371*(1708), 20160010. https://doi.org/10.1098/rstb.2016.0010

Stubbs, B., Thompson, T., Acaster, S., Vancampfort, D., Gaughran, F., & Correll, C. U. (2015). Decreased pain sensitivity among people with schizophrenia. *PAIN*, *156*(11), 2121–2131. https://doi.org/10.1097/j.pain.0000000000000304

Tabachnick, B. G., & Fidell, L. S. (2013). *Using Multivariate Statistics* (6th ed.). Pearson Education, Inc.

Takahashi, T., Kido, M., Sasabayashi, D., Nakamura, M., Furuichi, A., Takayanagi, Y., … Suzuki, M. (2020). Gray Matter Changes in the Insular Cortex During the Course of the Schizophrenia Spectrum. *Frontiers in Psychiatry*, *11*. https://doi.org/10.3389/fpsyt.2020.00659

Torregrossa, L. J., Amedy, A., Roig, J., Prada, A., & Park, S. (2022). Interoceptive functioning in schizophrenia and schizotypy. *Schizophrenia Research*, *239*(July 2021), 151–159. https://doi.org/10.1016/j.schres.2021.11.046

Torregrossa, L. J., Bian, D., Wade, J., Adery, L. H., Ichinose, M., Nichols, H., … Park, S. (2019). Decoupling of spontaneous facial mimicry from emotion recognition in schizophrenia. *Psychiatry Research*, *275*, 169–176. https://doi.org/10.1016/j.psychres.2019.03.035

Tournier, J.-D., Smith, R., Raffelt, D., Tabbara, R., Dhollander, T., Pietsch, M., … Connelly, A. (2019). MRtrix3: A fast, flexible and open software framework for medical image processing and visualisation. *NeuroImage*, *202*(January), 116137. https://doi.org/10.1016/j.neuroimage.2019.116137

Tsakiris, M., & De Preester, H. (Eds.). (2019). *The Interoceptive Mind: From homeostasis to awareness* (First). Oxford, UK: Oxford University Press.

Vos, T., Abajobir, A. A., Abate, K. H., Abbafati, C., Abbas, K. M., Abd-Allah, F., … Murray, C. J. L. (2017). Global, regional, and national incidence, prevalence, and years lived with disability for 328 diseases and injuries for 195 countries, 1990–2016: a systematic analysis for the Global Burden of Disease Study 2016. *The Lancet*, *390*(10100), 1211–1259. https://doi.org/10.1016/S0140-6736(17)32154-2

Wiebking, C., Bauer, A., de GRECK, M., Duncan, N. W., Tempelmann, C., & Northoff, G. (2010). Abnormal body perception and neural activity in the insula in depression: An fMRI study of the depressed "material me." *The World Journal of Biological Psychiatry*, *11*(3), 538–549. https://doi.org/10.3109/15622970903563794

Wojtalik, J. A., Smith, M. J., Keshavan, M. S., & Eack, S. M. (2017). A Systematic and Meta-analytic Review of Neural Correlates of Functional Outcome in Schizophrenia. *Schizophrenia Bulletin*, *43*(6), 1329–1347. https://doi.org/10.1093/schbul/sbx008

Wylie, K. P., & Tregellas, J. R. (2010). The role of the insula in schizophrenia. *Schizophrenia Research*, *123*(2–3), 93–104. https://doi.org/10.1016/j.schres.2010.08.027

Yee, C. M., Mathis, K. I., Sun, J. C., Sholty, G. L., Lang, P. J., Bachman, P., … Nuechterlein, K. H. (2010). Integrity of emotional and motivational states during the prodromal, first-episode, and chronic phases of schizophrenia. *Journal of Abnormal Psychology*, *119*(1), 71–

82. https://doi.org/10.1037/a0018475